Materials Advances

ROYAL SOCIETY OF CHEMISTRY

REVIEW

View Article Online
View Journal | View Issue

Cite this: *Mater. Adv.*, 2026, 7, 83

Graphene and its derivatives in supercapacitors: a comparative review

Pinky Sagar,[a] Iqra Reyaz Hamdani,[a] Tadzio Levato,[b] Vincenzo Giannini[b] and Gobind Das *[a]

Recent advancements in supercapacitor technology have garnered significant attention due to their possible applications in next-generation energy-storage systems. Among the various factors that influence device performance, the selection or modification of electrode-materials has been a crucial part. In particular, graphene and its derivatives have emerged as leading candidates owing to their high surface-area, higher electrical conductivity, stability and mechanical robustness. This review critically poses the role of structural tuning through doping, selection of electrolytes, and formation of composites with transition metal dichalcogenides (TMDs), and metal oxides (MOs) in graphene-based supercapacitors. These modifications not only enhance electrochemical performance by improving charge transport and ion diffusion but also address limitations including poor energy density and structural degradation. Moreover, the design of hierarchical porous architectures and nanoparticle–graphene composites offer further improvements in specific capacitance and cycling stability. In this review, fundamentals, type, mechanism, formulae, electrode materials, material properties, and electrochemical behaviors are discussed, along with an outlook on existing challenges and future opportunities in optimizing graphene and its derivative for high-performance supercapacitors.

Received 6th September 2025,
Accepted 11th November 2025

DOI: 10.1039/d5ma01017a

rsc.li/materials-advances

1. Introduction

The rising global energy demand, coupled with increasing environmental concerns, has intensified the need for clean, reliable, and efficient energy storage systems. The swift advancement of renewable energy sources such as solar and wind has made energy storage technologies vital for ensuring a stable balance between energy supply and demand.[1–3] Supercapacitors have emerged as a promising energy storage solution among various devices, because of their exceptional power density, quick charge–discharge capability, and long operational lifespan.[4,5] Unlike conventional batteries,

[a] *Department of Physics, Khalifa University of Science and Technology, P.O. Box 127788, Abu Dhabi, United Arab Emirates. E-mail: gobind.das@ku.ac.ae*
[b] *Technology Innovation Institute, P.O. Box 9639, Abu Dhabi, United Arab Emirates*

Pinky Sagar

Pinky Sagar received her MS degree from BBA, University, Lucknow, India in 2017 and PhD from Banaras Hindu University, Varanasi, India in 2023. After that, she had worked as a teaching fellow (2023–2024) and RJP-PDF (2024) at department of Physics, Banaras Hindu University, Varanasi, India. At present, she is working as a postdoctoral fellow at Khalifa University of Science and Technology, Abu Dhabi, UAE. Her research interests include advanced functional materials and devices for healthcare and energy storage applications.

Iqra Reyaz Hamdani

Iqra Reyaz Hamdani received her PhD degree from Indian Institute of Technology, New Delhi, India in 2020. Since then, she has been working as a postdoctoral fellow at Khalifa University of Science and Technology, Abu Dhabi, UAE. Her work integrates synthesis, characterization, and device fabrication to explore innovative solutions in energy and materials science.

supercapacitors can deliver energy in short bursts, which makes them ideal candidate for applications requiring quick energy release, such as electric vehicles, portable electronics, and backup power systems.[6,7] The performance of these devices, however, is largely governed by the characteristics of the electrode components used, driving intensive research into the development of advanced materials with superior electrochemical characteristics.[8–10]

Graphene-based supercapacitors have garnered remarkable interest owing to the unique amalgamation of graphene's idiosyncratic features and the growing demand for high-performance energy storage systems. Graphene, with its atomically thin structure, extraordinary electrical, thermal conductivity, high aspect ratio (surface to volume ratio), chemical inertness, and mechanical flexibility, offers a highly advantageous platform for supercapacitor electrodes. However, pristine graphene alone cannot fulfill all the necessities for practical energy storage, particularly in case of energy-density.[11,12] This has led to the development of composite materials, where graphene is combined with, other carbonous materials (activated carbon, carbon dots, *etc.*), transition metal di chalcogenides (TMDs) (MoS_2, WS_2, VS_2, *etc.*), metal oxides (MOs) (Fe_2O_3, SnO_2, CuO, NiO, *etc.*), conducting polymers, or other nanostructured materials to enhance its charge storage capabilities.[13–21] Understanding how these combinations influence electrochemical performance is crucial for engineering efficient, scalable, and cost-effective supercapacitor devices.[22,23] Given the ongoing global transition to cleaner energy technologies, advancing the field of graphene-based supercapacitors holds significant promise for applications in transportation and grid energy buffering. Hence, a systematic exploration of recent advancements, challenges, and prospects in this field is both timely and vital.

Till the date, substantial growth has been done in the synthesis and application of graphene-based electrodes for supercapacitors, with numerous studies demonstrating improved capacitance, cycling stability and rate capability, through the incorporation of metal oxides, conducting polymers, and hybrid nanostructures. Advances in fabrication techniques have enabled the design of novel architectures that maximize surface area and facilitate efficient ion transport.[24–26] Despite these advancements, several challenges remain unresolved. For instance, the restacking of graphene sheets often decreases, electrical conductivity and accessible surface area, limiting overall capacitance. Moreover, attaining uniform dispersion and firm interfaces between graphene and other composite materials is still difficult which may affect device reproducibility and long-term stability.[27–32] Large-scale productivity and cost-effectiveness of synthesis methods are also important concerns for commercial deployment. Moreover, fundamental understanding of charge storage mechanisms, especially in complex ternary or hybrid systems, is incomplete, hindering rational design. These knowledge gaps highlight the need for further research focusing on controlled material

Tadzio Levato

Tadzio Levato received his PhD degree from Università di Pisa-Scuola Galileo Galilei in 2007. At present he is director of Meta materials Group at Technology Innovation Institute, Abu Dhabi, UAE. His scientific interest focuses on Metamaterial production, nuclear plasma interactions, LASER material processing and smart materials.

Vincenzo Giannini

Vincenzo Giannini graduated in Physics from the University of Pisa and earned his PhD at the Spanish Research Council (CSIC) in Madrid. He pursued postdoctoral research in Amsterdam and held a Marie Curie Fellowship at Imperial College London. In 2014, he established his research group at Imperial's Condensed Matter Theory section, later joining CSIC in Spain and currently working at Technology Innovation Institute, Abu Dhabi, UAE. His scientific interests focus on theoretical light–matter interactions, including linear and nonlinear plasmonics, nanophotonics, and metamaterials, contributing significantly to the advancement of theoretical frameworks in these domains.

Gobind Das

Gobind Das is an Associate Professor at Khalifa University of Science and Technology, Abu Dhabi, UAE, since 2019. He previously served as a Scientist at KAUST, Saudi Arabia, focusing on plasmonic devices for biomedical applications. He holds a PhD in Physics from the University of Trento, Italy, and completed postdoctoral research at the University of Trento and Magna Graecia University, Italy. He also led a team at Istituto Italiano di Tecnologia. His expertise spans spectroscopy techniques (SERS, TERS, near-field imaging) and nanofabrication for biomedical and photonic applications. Dr Das has extensive experience in micro/nanofabrication and advanced spectroscopic characterization.

assembly, enhanced electrochemical characterization, and scalable fabrication processes to explore the maximum potential of graphene-based supercapacitors.

The current review is intended to provide a thorough and systematic overview of graphene and its derivatives including graphene oxide (GO), reduced graphene oxide (rGO), graphene quantum dots (GQDs), functionalized graphene and carbon nanotubes (CNTs) and their applications in supercapacitor technology. We begin by introducing the fundamentals of supercapacitors and then properties of graphene-based material. This covers the fundamentals and various catagories of supercapacitors, including electric double-layer capacitors (EDLCs), pseudocapacitors, and hybrid supercapacitors, along with the relevant electrochemical formulae and charge storage mechanisms. A significant focus is placed on the incorporation of other materials, including dopants, TMDs, and MOs, into graphene matrices to enhance electrochemical performance. The discussion extends to how these composite materials improve capacitance, stability, and charge–discharge rates by modifying surface area, conductivity, and redox activity. By covering synthesis strategies, material characterization, and performance evaluation, this review aims to highlight recent advances and identify promising directions for optimizing graphene-based supercapacitors in future energy storage applications.

2. Fundamentals and types of supercapacitors

Widely utilized for energy storage, supercapacitors offer remarkable performance. They are made up of active electrode materials, electrolyte and separator and current collectors. In these components, the electrode material plays a significant role in influencing the performance.[33–36] The electrochemical properties of various electrode materials used in supercapacitors are summarized in Fig. 1(a)–(c).

Supercapacitors are categorized into three types on the ground of energy storage mechanism: EDLCs, pseudocapacitors, and asymmetric supercapacitors (battery-type).

2.1 Electric double-layer capacitors (EDLCs)

Earlier, EDLCs dominated the supercapacitor landscape, operating on the principle of electrostatic interaction at the electrode–electrolyte boundary. In this process, electrons and ions used to accumulate at the top of active electrode material facilitating storage of energy.[38,39] Moreover, the energy storage capability of EDLCs is directly influenced through the factors such as surface area of the electrode material. It has been found that materials with a higher specific surface area offer higher numbers of attachment sites for electrons and ions, thus enhancing capacitance.[40,41] The earliest conceptual model of the EDLCs was introduced by Helmholtz, and is often called the Helmholtz double layer. Later refinements, such as the Gouy–Chapman and Gouy–Chapman–Stern models, provided more accurate representations of the EDLC's structure and behavior.

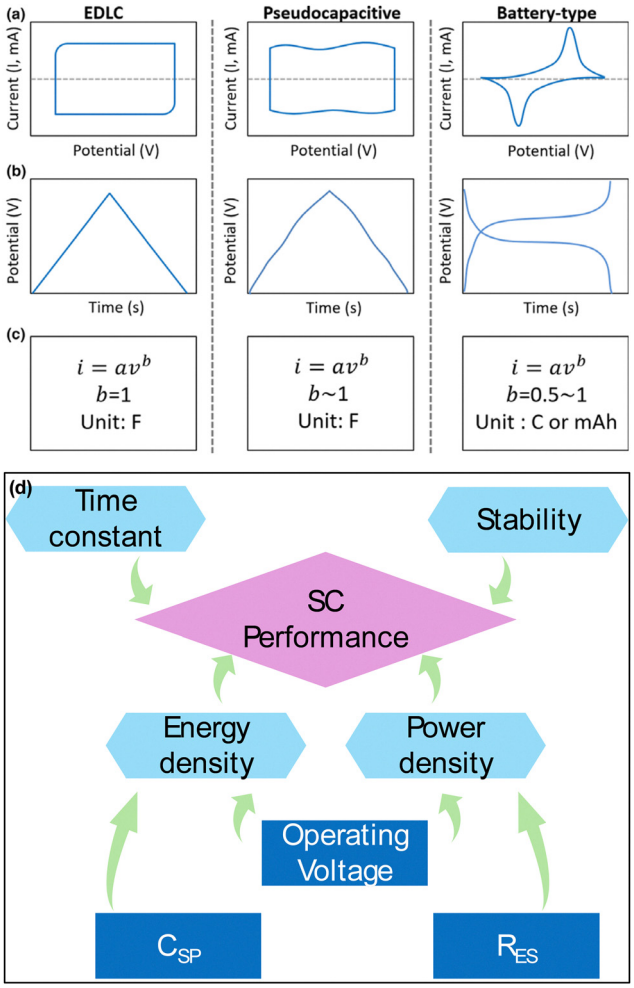

Fig. 1 (a)–(c) Categories of supercapacitors based on their energy storage mechanism. Reproduced with permission.[37] (d) Representation of key parameters affecting SC performance.

These devices typically use activated carbon (AC) as the electrode material due to its extremely high surface area, which allows for significantly greater charge storage. As a result, EDLCs are rated in Farads (F), in contrast to traditional capacitors, which are measured in picofarads (pF) or microfarads (μF).

Carbon-related materials including porous carbon, graphene, CNTs, activated carbon (AC) are considered perfect for EDLCs due to their high specific surface area, multi-channel structure, defects, oxygen rich sites, and excellent electrical conductivity.[42–45] Electrochemically, EDLCs exhibit a potential-independent capacitance during a voltage sweep, leading to a characteristic rectangular CV curve and a nearly constant current during charge/discharge cycles (Fig. 1a).[46–48]

2.2 Pseudocapacitors

Unlike EDLCs, pseudocapacitors follow rapid and reversible-redox reactions taking place at the electrode–electrolyte interface rather than purely physical ion accumulation. As a result, pseudocapacitors show widened peaks or minimal separation

in peak positions in CV curves.[49] The corresponding galvanostatic charge–discharge (GCD) curves exhibit two distinct behaviors: (i) segmented GCD curve: for bulk materials due to slow ion/electron diffusion and sluggish reaction kinetics, the GCD curve appears segmented; (ii) linear GCD curve: for ultrafine nanoparticles, faster ion/electron diffusion leads to improved reaction kinetics, resulting in a linear GCD curve.[49,50]

Metal-based materials (*e.g.*, nickel and cobalt compounds) with abundant redox-active sites are commonly used as pseudocapacitive electrodes. These materials provide elevated theoretical C_{sp} and are extensively employed in supercapacitors designed for high-energy-density applications.[51–53] However, a major drawback of pseudocapacitors is that their redox reactions are not fully reversible, leading to a gradual decline in cycling stability and capacitive performance for multiple charge–discharge cycles. Also, their lower conductivity and slow reaction kinetics limit their power density compared to EDLCs.[47,54]

2.3 Asymmetric supercapacitors (ASCs)

In the past few decades, ASCs have gained attention thanks to their ability to achieve high energy and power densities simultaneously. ASCs show combined behavior of battery and capacitive electrode components, which allow them to operate above the thermal decomposition voltage of electrolytes. This enhanced voltage window significantly improves energy storage capabilities.[55,56] ASCs, also referred to as battery-type supercapacitors, function through ion intercalation or phase conversion reactions, resembling the mechanism of batteries.[57] Their CV curves exhibit distinct faradaic redox peaks, with a larger voltage separation between oxidized and reduced states (typically 0.1–0.2 V), attributed to phase transitions. The constant-current charge–discharge curves of ASCs often display an obvious voltage plateau, confirming the presence of two phases.[58–60] Compared to conventional batteries and supercapacitors, ASCs-comprising both battery-type and capacitor-type materials-achieve an optimal balance between energy density and power density, making them highly promising for commercial applications.[57]

In ASC devices, gel electrolytes serve as a crucial component by enabling efficient ion transport between electrodes while offering enhanced mechanical stability and safety. Unlike liquid electrolytes, gel-based systems such as PVA–H_3PO_4 or PVA–KOH are semi-solid, which prevents leakage and supports flexible or solid-state configurations.[61] Their ability to maintain a wide electrochemical window contributes to higher energy density, and their compatibility with various substrates makes them ideal for wearable and portable electronics.[62] Overall, gel electrolytes improve the durability, flexibility, and electrochemical performance of ASC devices.

3. Mechanism and formulae

In practical applications, both EDLC and pseudocapacitance contribute to the overall charge storage capability of SCs, though their proportions vary depending on the materials used. For instance, in AC-based EDLCs, charge storage is primarily governed by the formation of electric double layers. However, the presence of oxygen-containing functional groups on the AC surface can also trigger surface redox reactions, adding a pseudocapacitive component.

To assess the performance of SCs, three key parameters are commonly used: total cell capacitance, operating voltage, and equivalent series resistance. These metrics are typically sufficient for evaluating commercial SC products, where the materials, manufacturing processes, and cell architecture are standardized. However, in research settings, where new materials, innovative fabrication techniques, and novel cell designs are constantly being explored, additional factors become essential for a comprehensive evaluation. A wide range of parameters must be considered to fully understand SC behavior.

An illustrative overview of the complex relationships among performance metrics, influencing factors, is presented in Fig. 1d. This diagram serves as a conceptual guide and does not aim to exhaustively cover all variables or their intricate interdependencies. For instance, it does not explicitly detail how operating voltage is measured or how electrolyte composition affects specific capacitance.

Electrochemical performance of supercapacitors is typically evaluated using either a two-electrode or a three-electrode setup. Key techniques used in these assessments include CV, GCD, and EIS. CV is commonly employed to estimate the gravimetric C_{sp} from the obtained voltammograms within a specific electrolyte environment.[63,64] The C_{sp} can be determined from either CV or GCD data using the following formula (eqn (1) and (2)):[65]

$$C_{sp} = \frac{\int i\mathrm{d}V}{2 \times m \times \Delta V \times S} \quad (1)$$

where C_{sp} is the specific capacitance measured from CV tests (F g^{-1}), $\int i\mathrm{d}V$ is the integrated area of CV curves, m is active the mass of loading material (g), ΔV is the potential window range (V), and S is the scan rate (V s^{-1}).

$$C_{sp} = \frac{I \times \Delta t}{m \times \Delta v} \quad (2)$$

Where C_{sp} is the specific capacitance measured from GCD curves (F g^{-1}), I represent the constant discharge current (A), m is active the mass of loading material (g), and Δv is the potential window range (V).

Apart from CV, EIS is a valuable technique for evaluating the capacitance of electrode materials. EIS involves applying a small alternating voltage (typically 5–10 mV) across a broad frequency range, usually from 0.01 Hz to 100 kHz.[66] Measurements are generally conducted at open-circuit potential. One of the key advantages of EIS is its ability to analyze the electrode's response by examining the relationship between the imaginary component of impedance ($|Z|$) and frequency (f). Unlike CV or GCD methods, capacitance through EIS can be derived from the Bode plot using the linear segment of the log $|Z|$ *versus* log$f$ curve, applying the formula $C = 1/(2\pi f|Z|)$. This analysis reveals

that capacitance is inversely related to frequency; as frequency increases, the measured capacitance tends to decrease.[67] At high frequencies, supercapacitors primarily exhibit resistive behavior, which is attributed to the movement of electrolyte ions.[48] This occurs because, at such frequencies, the relatively large size of the ions prevents them from accessing the micropores within the electrode material. In this region, the overall resistance reflects the combined conductivity of both the electrode material and the electrolyte.[68] In the intermediate frequency range, the impedance response often displays pseudo-charge transfer resistance, suggesting that the electrode material has a porous architecture. At low frequencies (typically below 1 Hz), the system demonstrates ideal capacitive behavior, which is a hallmark of efficient charge storage, as seen in the impedance spectrum.[69]

Energy density (eqn (3)) and power density (eqn (4)) are key parameters for assessing the performance of energy storage devices. These metrics provide insight into how much energy a device can store and how quickly it can deliver that energy. Energy and power densities are typically expressed either gravimetrically (per unit mass) or volumetrically (per unit volume). Power density, measured in W kg^{-1} or W L^{-1}, reflects how efficiently a system can absorb or deliver energy. Energy density, given in Wh kg^{-1} or Wh L^{-1}, indicates the total amount of electrical energy that can be stored or supplied. They are commonly calculated using the following equations:[70]

$$W = \frac{1}{2} C_{\text{meas}} V^2 \tag{3}$$

where W and V represent energy density and cell voltage, respectively, and

$$P = \frac{\mathrm{d}W}{\mathrm{d}t} \tag{4}$$

where P and t represent power density and the discharge time, respectively.

To facilitate meaningful comparisons across different energy storage technologies, a Ragone plot is often used (energy density (y) *vs.* power density (x)). This plot includes a diagonal line representing the characteristic time, which provides insight into how long a device can operate at its rated power. However, actual operating times can vary significantly depending on the discharge rate or load conditions, this phenomenon known as rate dependence.

Enhancing the energy density of supercapacitor electrodes primarily involves two effective strategies: developing electrode materials with a high specific surface area and selecting electrolytes that offer a wide potential window compatible with the electrode material.[71,72] Key electrochemical parameters such as specific capacitance, rate performance, and cycling stability are essential in evaluating the suitability of electrode materials for supercapacitor applications. These parameters are strongly influenced by factors such as the material's porosity, the number of electroactive sites, the ion transport pathways within the electrolyte, and the overall electrical conductivity of the electrode.[16,72] Among these factors, porosity plays a particularly significant role in determining electrode performance. It is governed by aspects like pore volume, pore shape, pore size distribution, and the effective surface area available for charge storage. While the Brunauer–Emmett–Teller (BET) surface area is commonly used to characterize porosity, the electrochemically active surface area is often more relevant for assessing performance, as BET surface area does not directly correspond to the area accessible to electrolyte ions during operation. However, studies focusing specifically on the influence of pore shape on electrochemical performance remain limited. In most prior research, attention has primarily been given to parameters like BET surface area, pore size distribution, and total pore volume.[16,22,39,73]

Another major and important factor is cyclic stability in SCs which refers to their ability to maintain capacitance and performance over repeated charge–discharge cycles, which is essential for long-term reliability.[74] This stability is majorly influenced by electrode materials where carbon-based structures offer durability, while hybrid composites like GO@PANI//AC enhance both capacitance and cycle life, achieving over 10 000 cycles with minimal degradation.[75–77] Further, electrolyte innovations, such as water-in-salt systems, have enabled supercapacitors to exceed 100 000 cycles with over 90% retention and broad temperature operability.[78,79] Asymmetric configurations and surface treatments further improve cycle life. Also, impedance plays a key role in stability by reflecting internal resistance and charge transfer efficiency; lower impedance values typically indicate better ion transport and reduced energy loss, which helps preserve performance over time. Stability is commonly assessed through capacitance retention, coulombic efficiency, and electrochemical impedance spectroscopy (EIS), which tracks changes in resistance and helps diagnose degradation mechanisms.[80,81]

4. Electrode materials

The performance of supercapacitors is primarily influenced by the nature of the electrode materials, the properties of the electrolytes, and the interactions at the electrode–electrolyte interface.[82,83] Carbon-based materials, such as graphene, carbon nanotubes (CNTs), and activated carbon, have been widely explored to enhance the capacitance in EDLCs due to their outstanding physical and chemical characteristics.[84–86] Among these, activated carbon is the most frequently used material in commercial supercapacitors, mainly because of its high surface area and cost-effectiveness.[87–90] However, its relatively low electrical conductivity limits its effectiveness in high-power applications. In contrast, CNTs have emerged as promising electrode materials for supercapacitors owing to their superior electrical conductivity and large, easily accessible surface area.[91,92] Nevertheless, a significant limitation arises from their tendency to aggregate into bundles, which restricts electrolyte ion diffusion within the electrode structure, thereby resulting in a reduced C_{sp}.[93]

Pseudocapacitors typically deliver higher C_{sp} and energy density compared to electric double-layer capacitors due to

the involvement of faradaic redox reactions. The rapid redox kinetics and enhanced C_{sp} of pseudocapacitive materials make them suitable candidates for energy storage applications.[54] Considerable research has been directed toward tungsten oxide-based nanostructures as promising pseudocapacitor electrodes because of their favorable morphology and electrochemical activity.[94] Additionally, transition metal oxides with variable oxidation states have gained attention for their ability to support efficient redox charge transfer processes, making them attractive materials for pseudocapacitor electrodes.[95] Conducting polymers have also emerged as a significant class of pseudocapacitive materials due to their tunable electrical conductivity and excellent environmental stability.[96,97] Regarding carbon-based materials, the pore diameter plays a critical role in ion accessibility; the pores must be sufficiently large to allow electrolyte ions to access the internal surfaces effectively. Smaller pore sizes can hinder ion transport and reduce capacitance. However, a direct correlation between specific surface area (SSA) and C_{sp} is not always evident, as other structural and electrochemical factors also influence performance (*cf.* Fig. 2).[98] For instance, Jian *et al.* engineered porous carbon nanosheet (CNS) for zinc-based hybrid supercapacitors, where they observed that micropores smaller than 6.0 Å can hinder the transport of hydrated Zn^{2+} ions, whereas those larger than 7.5 Å facilitate easier ion movement by presenting a lower energy barrier. Additionally, mesopores contribute to improved capacitance and rate performance by providing greater access to active sites and promoting efficient diffusion of hydrated Zn^{2+} ions. In Fig. 2, L-CNS and L-NS-CNS represent lignin-derived CNS and lignin-derived nitrogen/sulfur doped CNS having pore sizes 1–2.75 nm and 7–50 nm, respectively.[98]

4.1 Graphene and it's derivatives

Nanotechnology has evolved very vastly in sense of scientific exploration which offers immense potential across various domains. In the aspect of nanomaterials, each material with specific structural forms, surface characteristics, chemical compositions, and crystallographic arrangements has been engineered to meet the demands of specific applications such as energy storage. These tailored features enhance the stability, energy/power density and capacitance making nanomaterials indispensable in the development of advanced and reliable

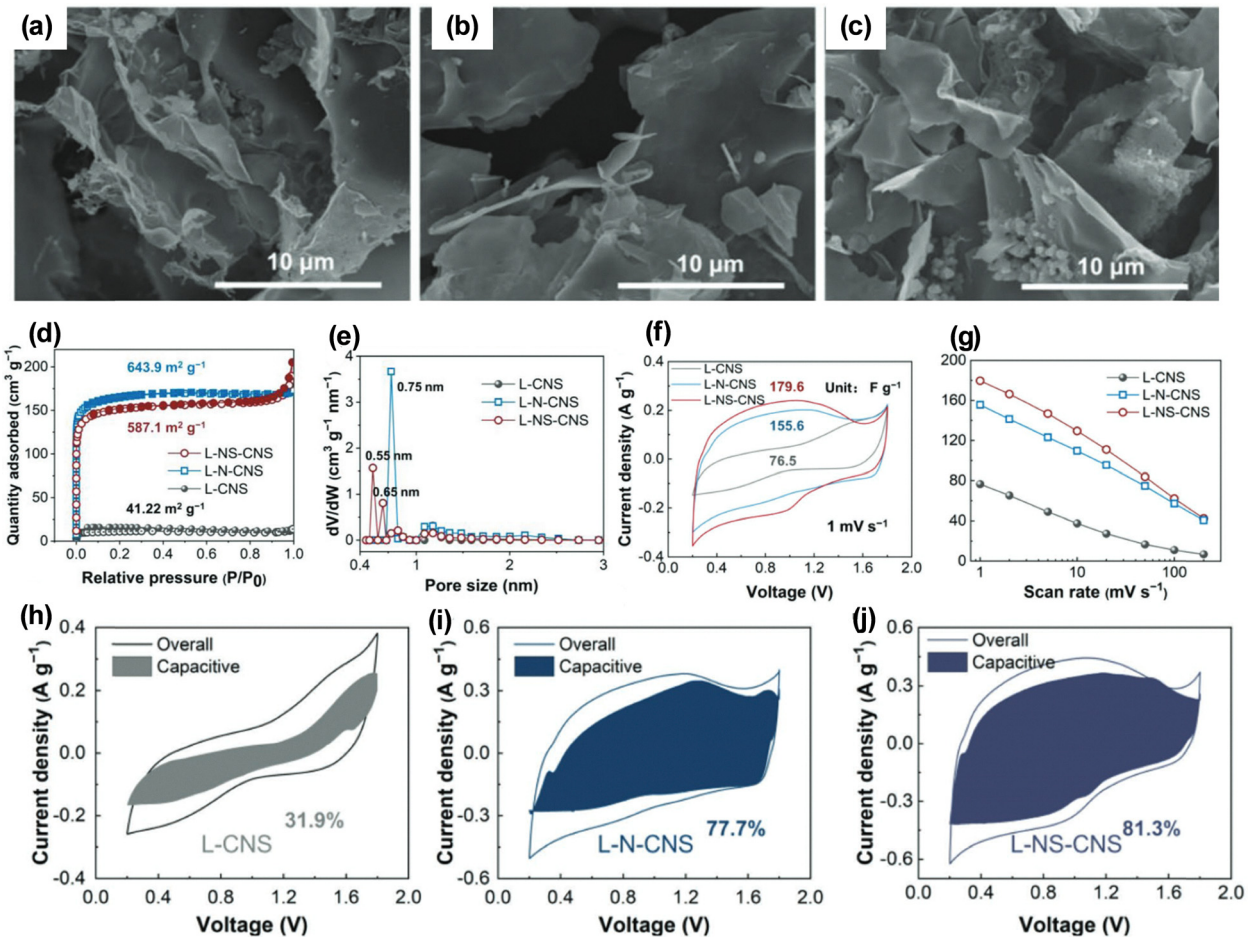

Fig. 2 SEM images of (a) L-CNS, (b) L-N-CNS, (c) L-NS-CNS. (d) N_2 adsorption/desorption isotherms, (e) pore size distributions. Electrochemical performances of L-CNS, L-N-CNS, and L-NS-CNS as the cathodes of ZIHCs: (f) CV curves at a scan rate of 1 mV s^{-1} (g) specific capacitances at scan rates ranging from 1 to 200 mV s^{-1}. Capacitive contribution calculated at a scan rate of 2 mV s^{-1} for (h) L-CNS, (i) L-N-CNS, and (j) L-NS-CNS, respectively. Reproduced with permission.[98]

energy storage technologies. Graphene, a single layer of carbon atoms arranged in a two-dimensional hexagonal lattice, has garnered significant attention for its exceptional properties and wide-ranging applications, including supercapacitors, HER, battery, CO_2-reduction and electrochemical sensing.[75,99–102] Its remarkable electrical conductivity ($\sim 10^8$ S m^{-1}), high thermal conductivity (2000–4000 W m^{-1} K^{-1}), impressive current density ($\sim 1.6 \times 10^9$ A cm^{-2}), and outstanding electron mobility ($\sim 200\,000$ cm^2 V^{-1} s^{-1}) make it a highly efficient material.[103] Additionally, graphene exhibits excellent mechanical strength, flexibility, transparency, and a broad electrochemical potential window, along with a high specific surface area. These properties enable rapid charge transport and efficient ion-diffusion, which are critical for high-performance energy storage. Its high specific surface area, mechanical strength, flexibility, and wide electrochemical potential window further enhance its suitability for supercapacitor electrodes.[104–107] For example, high surface area is beneficial for EDLCs as it supports enhanced charge accumulation. Graphene's maximum theoretical specific capacitance has been estimated to be around 550 F g^{-1}, assuming full utilization of the surface area.[108,109] Additionally, graphene itself has garnered significant attention as an anode material for lithium-ion batteries (LIBs) due to its notably high theoretical capacity, exceeding 670 mAh g^{-1}. Together, these properties highlight graphene's immense potential in achieving efficient ion and electron transport, which are critical features for high-performance supercapacitor electrodes.

Despite its exceptional theoretical potential, the actual capacitance values observed for graphene-based electrodes are typically much lower than predicted. This discrepancy arises primarily because theoretical estimations assume an ideal case of defect-free, monolayer graphene, which is not achievable under most practical conditions.[11] In real-world applications, multiple graphene layers are required to fabricate electrodes with sufficient mass loading, but this leads to restacking of the sheets. Such restacking-driven by π–π interactions between adjacent layers-significantly reduces the ion-accessible surface area, thereby limiting the formation of a robust EDLC and ultimately lowering the overall capacitance.[110] Additionally, while structural defects in graphene can aid in ionic diffusion and transport, they often come at the expense of electrical conductivity. Moreover, graphene's zero bandgap and hydrophobic nature can limit its interaction with electrolytes and reduce its electrochemical activity. Consequently, graphene electrodes face three primary challenges in SC applications: reduced accessible surface area, diminished conductivity, and lower-than-expected capacitance. These limitations must be addressed to realize the full potential of graphene in high-performance SC devices. To address these limitations, GO has been developed through oxidation of graphite, typically using the Hummers' method. GO incorporates oxygen-containing functional groups such as hydroxyl, epoxy, and carboxyl, which improve its dispersibility in aqueous media and allow for functionalization with other active materials. Moreover, GO offers a tunable bandgap and retains a high surface area, making it a versatile and cost-effective alternative for supercapacitor electrodes.

In most reported studies, graphene-based electrodes are synthesized through an oxidation–reduction process also, which typically involves converting natural graphite into GO, followed by chemical or thermal reduction to obtain reduced rGO.[111] However, this approach introduces structural defects and oxygen-containing functional groups, which substantially hinder the electrical conductivity of the resulting rGO material. As a result, such imperfections can negatively affect the power density and rate performance of the fabricated supercapacitor devices. Furthermore, the presence of these defects, along with the tendency of rGO sheets to restack, contributes to a reduction in accessible surface area, which in turn weakens ion adsorption capacity and electron transport pathways.[112] Together, these factors lead to a noticeable decline in the specific capacitance and overall performance of graphene-based supercapacitor electrodes. Other than pure graphene, porous carbon materials, including activated carbon, carbon aerogels, carbon nanotubes, carbide-derived carbon, and metal doping, are widely used as electrode materials in supercapacitors.[113–119]

Extensive research has been devoted to the commercial production of graphene. Various synthesis techniques have been developed, such as chemical vapor deposition (CVD), epitaxial growth on silicon carbide (SiC), chemical transformation processes, carbon monoxide reduction, and the unzipping of carbon nano tubes (CNTs).[44,120–122] Among these, CVD is widely utilized with metals like iron, copper and nickel serving as catalysts. However, not all fabrication methods are ideal for applications requiring consistent graphene quality. For instance, mechanical or chemical exfoliation of graphite powder yields graphene flakes that often lack uniformity. Epitaxial growth on SiC is another technique known for generating high-quality graphene, although it faces challenges in scaling up for large-area applications. CVD also produces high-grade graphene, though typically in limited quantities. In supercapacitor applications, rGO serves as an alternative. GO is generally synthesized from graphite using wet chemical processes, and its electrical properties can be improved through thermal treatment or solution-based reduction, which is visually marked by a color shift from brown to black.[123,124]

CVD is widely recognized for producing graphene with high quality and minimal defects. Currently, it stands out as one of the most cost-effective and scalable methods for fabricating graphene over large areas. Gaining insight into the atomic-level growth mechanisms during CVD can significantly aid in optimizing the quality of the resulting graphene.[125] However, current experimental methods fall short in revealing atomic-scale details of the growth process. Among chemical synthesis approaches, the reduction GO remains a straightforward and scalable method, making it a practical option for industrial-scale graphene production.[126,127] In CVD systems, the reaction temperature necessary for graphene growth is usually achieved through convection and radiation heat transfer between the heat source and the metal catalyst. While effective, this method

often suffers from low energy efficiency and prolonged synthesis durations. To address these limitations, Lin *et al.* developed an advanced CVD system capable of stabilizing the growth of bifacial graphene. This method enables the synthesis of high-purity graphene while effectively preventing contamination from oxygen, moisture, and intermediate by-products.[128] In another advancement, An *et al.* employed acid employed hydrothermal synthesis root to fabricate 3D graphene electrode for supercapacitor applications. As a result, they successfully obtained 3D graphene structure with specific surface area is 159.3 $m^2\ g^{-1}$ and porosity of 3–70 nm.[129]

Synthesis of graphene using bio-waste and bio-mass derived has been also a popular topic among researchers. For example, Yan *et al.* demonstrated synthesis of GO using milled miscanthus particles through pyrolysis method. They obtained amorphous GO with and aliphatic structures.[130] Li *et al.* synthesized graphene mixed and graphene-welded activated carbon (GMAC and GWAC, respectively) by a self-sustained combustion synthesis where they used CO_2 as a precursor for graphene and activated carbon as matrix. Hence derived GMAC and GWAC were further compared in terms of specific supercapacitance. GWAC demonstrated the highest specific capacitance ($\sim$150 F g^{-1}), confirming its superior performance as a supercapacitor electrode compared to AC, graphene, and GMAC. The superior performance of GWAC is attributed to its high surface area, excellent electrical conductivity, and optimized porous structure achieved through CO_2-assisted combustion synthesis.[131] In another report, Le *et al.* proposed an approach to improve the performance of graphene EDLCs by introducing ferroelectric polymers. In this work, they grew graphene using CVD approach on Cu foils at 1000 °C. The full-cell capacitor was attained by sandwiching two PEN/graphene/PVDF/graphene electrodes with H_3PO_4/PVA gel electrolyte (*cf.* Fig. 3) and reported enhancement in specific capacitance (36%) and potential window (1.0 V to 1.5 V).[132] Mesopores and structural support play pivotal roles in enhancing the supercapacitive performance of electrode materials. For instance, Zhao *et al.* reported multiholed graphene and carbon nanotube combination doped by nitrogen (GNCs) for supercapacitor applications (Fig. 4). Accordingly, GNCs supercapacitor demonsatrtes a high specific capacitance of 147 F g^{-1} at a current density of 1 A g^{-1}, along with excellent rate performance (110 F g^{-1} at 10 A g^{-1}), impressive cycling stability with 81.9% capacitance retention over 10 000 cycles at 5 A g^{-1}, and delivers a notable energy density of 16.8 Wh kg^{-1} at a power density of 14.4 kW kg^{-1}.[134] Mesopores (2–50 nm in size) provide efficient ion diffusion pathways, enabling rapid electrolyte transport and minimizing ion diffusion resistance (Fig. 4). This leads to improved charge/discharge rates and better utilization of the active material. Structural support, often provided by frameworks like CNTs or graphitized networks, ensures mechanical stability, preserves the integrity of the electrode during long cycling, and enhances electrical conductivity (Table 1). Together, these features result in high specific capacitance, superior rate capability, and excellent cycling stability. Corriea *et al*. and Imbrogno *et al*. found that laser-induced technique can also enable direct, cost-effective conversion of parylene-C into porous graphene films with low sheet resistance which is suitable for flexible electronics. It also allows one-step fabrication of ultrathin microsupercapacitors with excellent electrochemical performance and cycling stability (Fig. 5).

5. Composite formation

Electrode materials are fundamental to the performance and longevity of supercapacitors, significantly influencing both their capacitance and cycle stability. Beyond graphene and derivatives, other key materials under investigation for electrode applications include transition metal dichalcogenides (TMDs), metal oxides (MOs), metal–organic frameworks (MOFs), covalent organic frameworks (COFs), MXenes (transition metal carbides and nitrides), carbon-based materials, and transition metal oxides. Despite their promising potential in electrochemical energy storage, achieving a balance of desirable properties-such as a high surface area, structural robustness, low internal resistance, and efficient charge transfer, remains a major challenge.

To address these limitations, composite materials have been developed using various fabrication strategies. These composites combine the strengths of individual components while mitigating their weaknesses and often exhibit synergistic interactions. For instance, at heterogeneous interfaces, charge redistribution can create internal electric fields that enhance ion mobility. Additionally, the presence of lattice stress fields can help reduce mechanical deformation during electrochemical cycling, thus improving structural durability. As a result, graphene-based composites have gained considerable attention for energy storage applications due to their significantly enhanced electrochemical performance.

5.1 TMDs and graphene composites

TMDs, with the general formula MX_2 (where M = Mo or W and X = S or Se), have recently emerged as promising materials for a range of applications, including sensing,[183–187] water splitting,[188] catalysis,[189] and energy storage.[190,191] These compounds possess a layered structure similar to that of graphene, where the metal and chalcogen atoms are bonded covalently within the layers, while the layers themselves are held together by weak van der Waals forces (see Fig. 6a). This structural configuration not only resembles graphene but also facilitates the reversible intercalation and deintercalation of various electrolyte ions, making them highly suitable for energy storage devices.[192] For example, Bongu *et al.* reported that the MoS_2@graphene (1 : 9) electrode exhibited the highest specific capacitance of 248 F g^{-1} at a current density of 5 A g^{-1}, among other compositions, indicating superior electrochemical performance in supercapacitor applications. Accordingly, the specific capacitance was enhanced $\sim$6.2 times when compared with bare graphene ($\sim$40 F g^{-1}).[151] Devices in harsh environments: military, automotive, biomedical, oil exploration, and space,

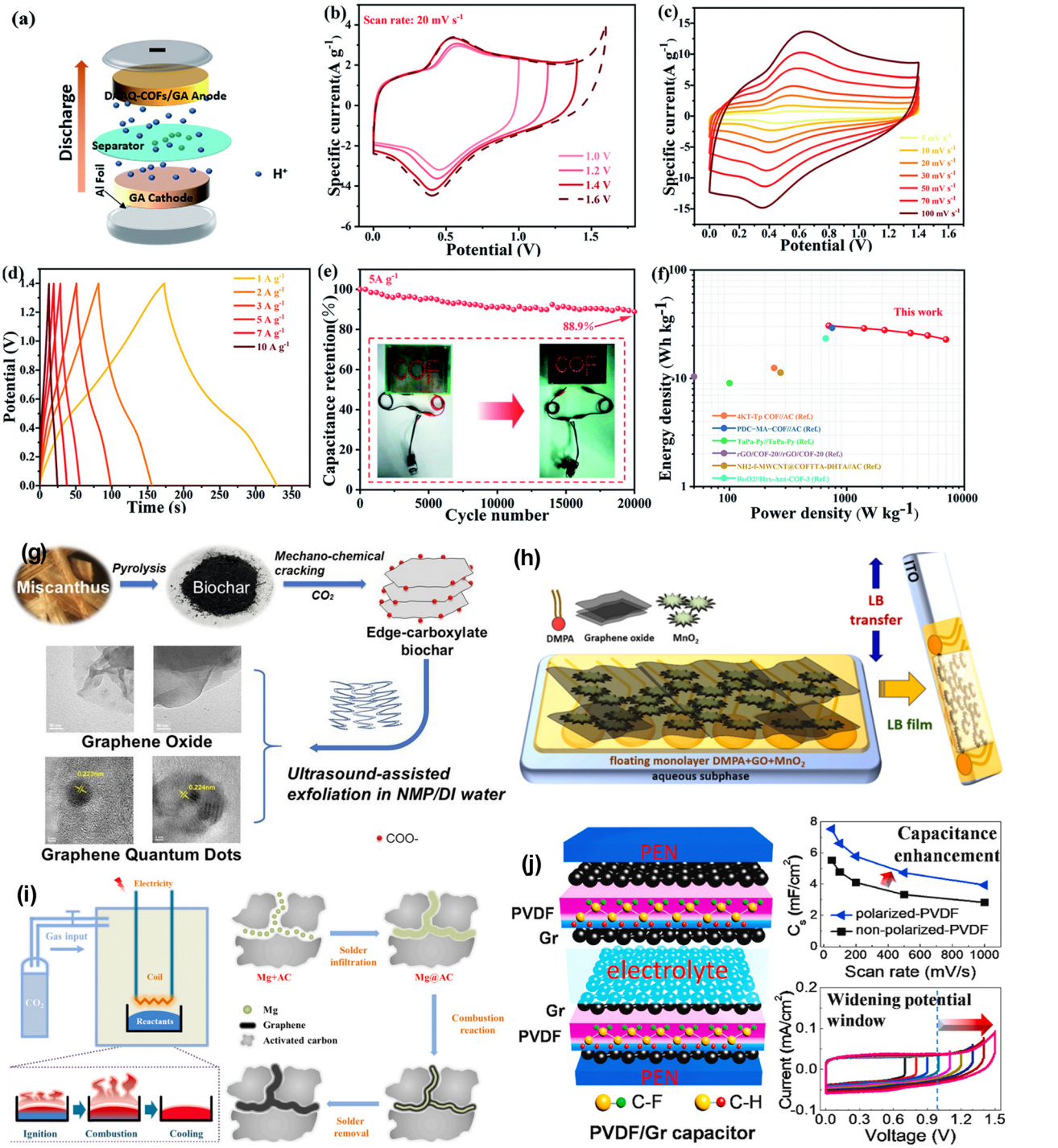

Fig. 3 Electrochemical performance characteristics of the anthraquinone-based covalent organic framework/graphene aerogel (DAAQ-COFs/GA) ASC: (a) schematic illustration of the ASC device. (b) CV curves recorded at 20 mV s^{-1} across different voltage windows. (c) CV profiles of the ASC at varying scan rates. (d) GCD curves at multiple current densities. (e) Long-term cycling stability at 5 A g^{-1} over 20 000 cycles (inset: image of LEDs illuminated using the DAAQ-COFs/GA ASC). (f) Ragone plot represents energy and power density characteristics of the ASC. Reproduced with permission.[129] (g) Synthesis of GO and GQDs from miscanthus *via* ultrasound-assisted mechano-chemical cracking. (h) Fabrication process for a LB film containing a hybrid nanostructure of DMPA + GO/MnO_2 on an ITO electrode. (i) CS process to prepare GWAC using Mg as sacrificial solder and graphene welding during the combustion of Mg in CO_2. (j) Polarised PVDF graphene capacitor along with specific capacitance comparison graph and CV. Reproduced with permission.[130–133]

must endure extreme temperatures, vibrations, moisture, and electromagnetic fields. Meeting these demands requires innovative designs and advanced materials to ensure reliability, durability, and performance under severe conditions. For instance, Serrapede *et al.*, documented a combination of MoS_2 with 3D graphene aerogel with promising capacitive

behavior (210 F g^{-1}) at high temperature (200 °C) which is 20% higher than existing literature. This device delivers an energy density of 0.22 Wh dm^{-3} in coin-cell form, significantly surpassing commercially available devices rated for up to 175 °C. It also operates reliably across a broad temperature range of 25 °C to 250 °C, with minimal performance variation.[152] In another article, Sardana *et al.* reported flower-like morphology of MoS_2@rGO nanohybrid using hydrothermal synthesis route. The MoS_2@rGO nanohybrid exhibited a high specific capacitance of 2049.90 F g^{-1} at a current density of 30 mA g^{-1} and demonstrated nearly 100% capacitance retention over 10^4 consecutive charge–discharge cycles at 660 mA g^{-1}. The exceptional electrochemical behavior arose from the unique 2D architecture of the MoS_2@rGO nanohybrid, characterized by its minimal equivalent series resistance and distinctive layered morphology.[153] In another report, Zhuo *et al.* reported 2D graphene produced *via* electrochemical exfoliation in acidic medium. As result, produced graphene with 1T-MoS_2 was utilized to fabricate supercapacitor electrode. This 2D electrode showed high specific capacitance of 290 F cm^{-3} at 0.5 A g^{-1} with ~90% retention of capacitance after 10^4 cycles.[193] Magdum *et al.* showcased 3D skeleton rGO/VS_2/WS_2 composite in hydrogel form. They reported that upon incorporation of VS_2/WS_2 into the specific capacitance of rGO enhanced significantly due to the porous structure of 3D skeleton rGO/VS_2/WS_2 composite. Hydrogel electrodes composed of rGO, rGO/VS_2, and a rGO/VS_2/WS_2 composite were fabricated binder-free on nickel foam (current collectors) using a hydraulic press. Among these, the rGO/VS_2/WS_2 composite hydrogel electrode demonstrated superior supercapacitive performance, achieving a specific capacitance of 220 F g^{-1} at a current density of 1 A g^{-1} in a 3 M KOH electrolyte. This performance surpassed that of the GO hydrogel (158 F g^{-1}) and the rGO/VS_2 hydrogel (199 F g^{-1}) under identical testing conditions.[181] In another report, Mashkoor *et al.* highly durable and free-standing supercapacitor using WS_2 and MWCNT nanocomposite as shown in Fig. 6b–j. The WS_2–MWCNT composite exhibited outstanding supercapacitive performance. The assembled device achieved a specific capacitance of 134.72 F g^{-1} at a current density of 6 A g^{-1} and delivered a notable energy density of 46.15 Wh kg^{-1} at a power density of 500 W kg^{-1}.[182] When combined with TMDs in electrode design, the TMD component typically contributes to pseudocapacitance, while the graphene material enhances the electrical conductivity and offers a high surface area for active charge storage. For example, anchoring NiS_2 nanoparticles and MoS_2 nanosheets onto graphene layers expose numerous active edge sites and defects. In this configuration, graphene not only contributes to enhanced capacitance but also promotes efficient electron transport. A device using a NiS_2/MoS_2/graphene composite as the anode and nitrogen-doped porous graphene as the cathode demonstrated an impressive energy density of 84.5 Wh kg^{-1} in aqueous electrolyte (2 M KOH). Benefitting from NiS_2/MoS_2/graphene's exclusive chemical properties and structure, it demonstrates impressive electrochemical performances for battery-type supercapacitors in terms of high specific capacity of 2379 F g^{-1} at 1 A g^{-1} with significant rate capability (60.7% at 100 A g^{-1}).[158] The introduction of TMD nanosheets between graphene layers effectively reduced the tendency of graphene sheets to restack, thereby enhancing the overall structure. This intercalation not only boosted the pseudocapacitance contributed by NiS_2/MoS_2 but also improved the electrochemical

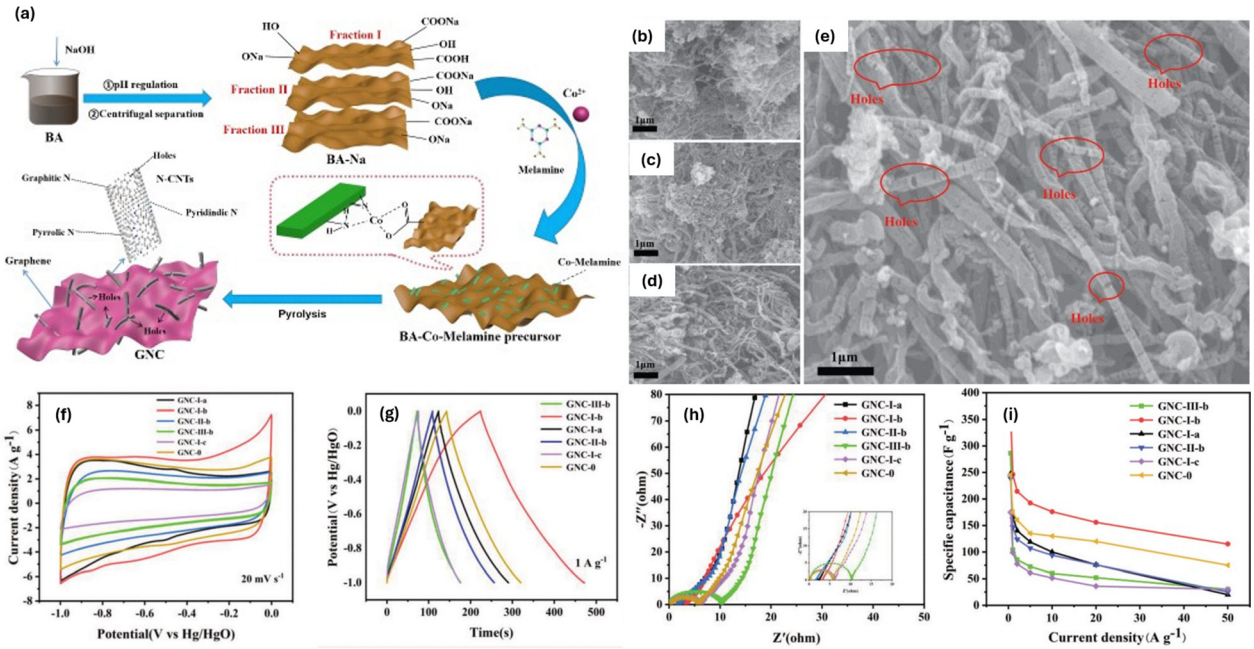

Fig. 4 (a) Schematic representation of synthesis of GNC, (b)–(e) SEM images of GNC, (f) CV curves (g) GCD curves (h) EIS spectra and (i) specific capacitances at various current densities. Reproduced with permission.[134]

Table 1 Summary of application of graphene and graphene derivative materials as electrodes in supercapacitors

Material	Electrolyte	Pore size/ volume	Surface area	Specific capacitance@current density	Energy density	Ref.
Graphene	PVA	0.02281 cm^3 g^{-1}	4.6 ± 0.026 m^2 g^{-1}	1.56 mF cm^{-2} (planer) and 3.77 mF cm^{-2} (sandwich)@0.1 mA cm^{-2}	1.7 μWh cm^{-2}	135
Graphene	PVA/H_2SO_4	—	—	1.66 mF cm^{-2}@(0.5 mA cm^{-2}	0.19 μWh cm^{-2}	136
Graphene	PVA–table sea salt	—	—	31.67 F g^{-1}@0.25 A g^{-1}	6.33 Wh kg^{-1}	137
GQDs	KOH	—	—	200 F g^{-1}@2.0 A g^{-1}		22
PEN/graphene/PVDF/ graphene	H_3PO_4/PVA	—	—	75 F cm^{-3}@1 μA cm^{-2}		132
CuS|P-CuGFs	KOH	—	—	1460.9 mF cm^{-2}@3 mA cm^{-2}	15.3 μWh cm^{-2}	138
GO	PVA/H_2SO_4	—	179 m^2 g^{-1}	471 F g^{-1}@0.2 A g^{-1}	48.18 Wh kg^{-1}	139
rGO	KOH	—	—	232 F g^{-1}@0.5 A g^{-1}	21 Wh kg^{-1}	140
rGO	Na_2SO_4	—	—	176 F g^{-1} 0.5 A g^{-1}	47 Wh kg^{-1}	141
rGO/PPy	PVA/KOH	3 nm	168.91 m^2 g^{-1}	422.6 F g^{-1}@0.5 A g^{-1}	58.7 Wh kg^{-1}	142
rGO/PPy	PVA/H_2SO_4	—	79 m^2 g^{-1}	1532 mF cm^{-2}@0.88 mA cm^{-2}	114 μWh cm^{-2}	143
rGO/PPy	Na_2SO_4	—	74.0 m^2 g^{-1}	389.3 F g^{-1}@1.0 A g^{-1}	19.7 Wh kg^{-1}	144
rGO/PPy	KCl/pyrrole	—	23.1 m^2 g^{-1}	414 F g^{-1}@0.2 mA cm^{-2}	—	145
rGO	COP	—	—	417 F g^{-1}@0.81 A g^{-1}	86.4 Wh kg^{-1}	146
$MnFe_2O_4$@rGO	KOH	—	—	399.17 F g^{-1}@0.65 A g^{-1}	40.05 Wh kg^{-1}	147
$NiFe_2O_4$/r-GO	KOH	—	—	362.46 F g^{-1}@0.65 A g^{-1}	36.37 Wh kg^{-1}	148
N doped graphene	KOH	—	114.6 m^2 g^{-1}	152.8 μF cm^{-2}@1 A g^{-1}	16.9 Wh kg^{-1}	149
Cl^- doped graphene	EMIMBF$_4$/PVDF-HFP	2 nm	238.8 m^2 g^{-1}	160 F cm^{-3}	97.9 mWh cm^{-3}	150
B doped graphene	PVA	0.02281 cm^3 g^{-1}	4.6 ± 0.026 m^2 g^{-1}	4.67 mF cm^{-2} (planer) and 11.24 mF cm^{-2} (sandwich)@0.1 mA cm^{-2}		135
MoS_2@graphene	KOH	>5 nm	85 m^2 g^{-1}	248 F g^{-1}@5 A g^{-1}	—	151
MoS_2@rGO	BMIM BF$_4$	—	—	217 F g^{-1}	0.22 Wh dm^{-3}	152
MoS_2@rGO	Na_2SO_4	0.82 nm	7.74 m^2 g^{-1}	2049.90 F g^{-1}@30 mA g^{-1}	192.43 Wh kg^{-1}	153
MoS_2@graphene	PVA (poly(vinyl alcohol))/H_2SO_4	—	—	1.8 mF cm^{-2}	0.156 μWh cm^{-2}	154
WS_2@graphene	Na_2SO_4	2 nm	761 m^2 g^{-1}	2964 mF cm^{-2}	—	155
WS_2@graphene	H_2SO_4	—	—	421.5 F g^{-1}@1 A g^{-1}	~10 Wh kg^{-1}	156
WS_2-embedded MXene/GO	KOH	—	12.97 m^2 g^{-1}	1111 F g^{-1}@at 2 A g^{-1}		31
WS_2/rGO/CNT	pDADMTFSI and PYR$_{14}$TFSI	—	—	67.60 F g^{-1}@135.93 mA cm^{-3}	115.01 Wh kg^{-1} or 8.50 mWh cm^{-3}	157
NiS_2/MoS_2/graphene	KOH	—	155 m^2 g^{-1}	2379 F g^{-1}@1 A g^{-1}	84.5 Wh kg^{-1}	158
β-Ni(OH)$_2$/graphene	$(NH_4)_2SO_4$	—	—	61.7 mF cm^{-2}@5 mA cm^{-2}		30
GO/Fe_3O_4	PANI	—	—	283.4 F g^{-1}@1.0 A g^{-1}	47.7 Wh kg^{-1}	159
MnO_2–rGO	H_2SO_4/PVA	—	—	103 F g^{-1}@0.75 A g^{-1}	41.5 Wh kg^{-1}	160
Co–CeO_2/rGO	Na_2SO_4	—	—	594.3 F g^{-1}@0.25 A g^{-1}	27.13 Wh kg^{-1}	161
AGO	H_2SO_4	—	—	3890 F g^{-1}@2 A g^{-1}	540.71 Wh kg^{-1}	162
Ag–rGO@CuO	KOH			612.5 F g^{-1}@0.5 A g^{-1}	—	163
NiO/CuO/rGO	Na_2CO_3	9–27 nm	392 m^2 g^{-1}	531.56 F g^{-1}@1 A g^{-1}	170.09 Wh kg^{-1}	164
ZnO–CuO/rGO	H_2SO_4	7.1 nm	128.18 m^2 g^{-1}	270.6 F g^{-1}@0.5 A g^{-1}	6.2 Wh kg^{-1}	165
Cl^- GO@CuO/Cu_2O	KOH	—	0.064 cc g^{-1}	577 F g^{-1}	25.3 Wh kg^{-1}	166
GQDs/CuO	KOH	5–21	101.2 m^2 g^{-1}	729 F g^{-1}@1 A g^{-1}	32.2 Wh kg^{-1}	167
GO–CuO	KOH	—	—	82.1 F g^{-1}@0.5 A g^{-1}	—	168
CuO–Cu_2O/graphene	Na_2SO_4	—	—	1589 F g^{-1}@2 A g^{-1}	3.8 μWh cm^{-2}	169
rGO/CuO/PpPD	H_2SO_4	—	—	512.12 F g^{-1}@1 A g^{-1}	—	170
CuO–rGO	KOH	—	—	188 F g^{-1}@0.2 A g^{-1}	7.32 Wh kg^{-1}	171
PPY:CuO:rGO	H_2SO_4	—	—	850.12 F g^{-1}@2.8 A g^{-1}	16.56 Wh kg^{-1}	172
FeO–CuO–RGO	—	0.76 and 1.32 nm	168 m^2 g^{-1}	626 F g^{-1}@1 A g^{-1}	86.94 Wh kg^{-1}	173
Fe–PrGO	KCl	—	128 m^2 g^{-1}	442 F g^{-1}@1 A g^{-1}	61.39 Wh kg^{-1}	174
rGO–Cu	KCl	—	—	208.9 F g^{-1}	—	175
Graphene/Cu_2O	KOH	—	—	161.31 F g^{-1}@1 A g^{-1}	6.63 Wh kg^{-1}	176
Fe_2O_3/rGO/PPy	H_2SO_4	—	—	158.2 F g^{-1}@1 A g^{-1}	87.05 Wh kg^{-1}	177
rGO–CuO	KOH	4–10 nm	60.02 m^2 g^{-1}	712 F g^{-1}@1 A g^{-1}	—	178
α-Fe_2O_3/rGO	PVA/KOH	—	18.3 m^2 g^{-1}	455 F g^{-1}@1 A g^{-1}	73 Wh kg^{-1}	179
rGO/Fe_2O_3	KOH	—	184 m^2 g^{-1}	360 F g^{-1}@1 A g^{-1}	—	180
rGO/VS_2/WS_2	KOH	—	—	220 F g^{-1}@1 A g^{-1}	30.55 Wh kg^{-1}	181
WS_2–MWCNT	Na_2SO_4			134.72 F g^{-1}@6 A g^{-1}	46.15 Wh kg^{-1}	182

PEN = polyethylene naphthalate; PVDF = polarized poly(vinylidene fluoride); pDADMTFSI = poly(diallyldimethylammonium) bis (trifluoromethanesulfonyl)imide; PYR$_{14}$TFSI = *N*-butyl-*N*-methylpyrrolidinium bis(trifluoromethylsulfonyl)imide; CuS|P-CuGFs = copper coated graphene fibers; COP = poly(pyrrole-*co*-thiophene); AGO = copper oxide decoratedamine functionalized graphene oxide; PANI = polyanailine; GQDs = graphene quantum dots; PpPD = poly(*p*-phenylenediamine); PPY = polypyrrole; Fe–PrGO = iron oxide embedded polypyrrole-rGO matrix; PVA = polyvinyl alcohol.

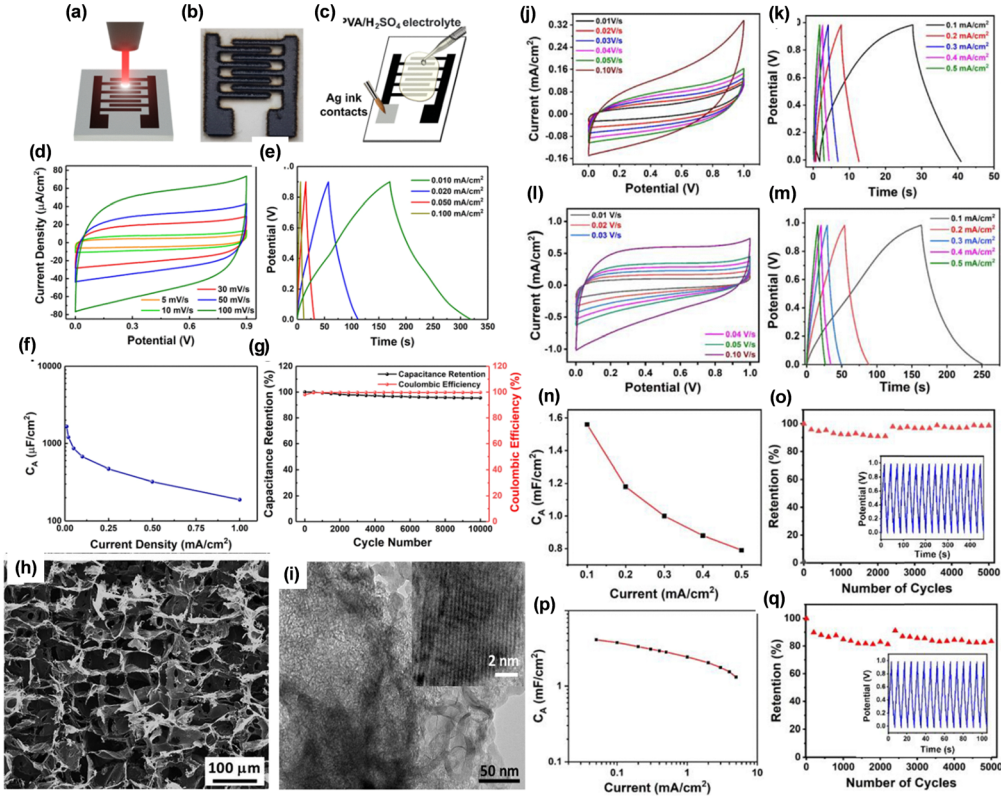

Fig. 5 (a) Illustration of the direct laser writing process used to fabricate micro-supercapacitor (MSC) electrodes or laser induced graphene (LIG); (b) LIG-MSC electrodes patterned directly onto a parylene-C substrate; (c) schematic showing the structural assembly of the LIG-MSC device; (d) CV curves demonstrating electrochemical behavior; (e) charge–discharge profiles at various current densities; (f) specific capacitance values as a function of current density; and (g) long-term cycling stability and Coulombic efficiency at 0.5 mA cm^{-2} for the LIG-MSCs fabricated on parylene-C. Reproduced with permission.[136] (h) SEM image of image of the LIG graphitized area, (i) TEM image of LIG. (j) CV of a representative open LIG device, (k) GCD curves of open LIG device (l) CV of a sandwich LIG device (m) GCD curves of sandwich LIG device. (n) Plot of area capacitance (C_A) *vs.* current density for open LIG device and corresponding (o) cycling stability over 5000 cyles. (p) Plot of area capacitance (C_A) *vs.* current density for sandwich LIG device and corresponding (q) cycling stability over 5000 cyles. Reproduced with permission.[135]

double-layer capacitance primarily offered by graphene. The resulting NiS_2/MoS_2/graphene nanocomposite exhibited superior electrochemical performance compared to pure graphene. Moreover, optimizing the proportion of TMDs in the composite further enhanced the volumetric capacitance of the supercapacitor.

5.2 MOs and graphene composites

The enhanced supercapacitive performance of graphene or graphene oxide (GO/rGO) combined with metal oxides arises from the interplay of electrostatic and faradaic charge storage mechanisms.[13] Graphene-based materials contribute to EDLC by forming electric double layers at the electrode–electrolyte interface, governed by classical electrostatics and supported by graphene's large surface area and excellent conductivity for rapid electron transport.[11,195] MOs introduce pseudo capacitance through fast, reversible redox reactions at or near the surface, enabling bulk charge storage *via* quantum electron transfer and ion intercalation, as described by faradaic processes.[54,95,173,174,196] The hybridization enhances quantum capacitance by increasing the density of electronic states near the Fermi level, particularly when functional groups or defects are introduced. MOs also improve ionic conductivity and ion diffusion by offering porous, nanostructured pathways governed by Fick's laws, while graphene ensures continuous conductive networks. This synergy results in high specific capacitance, improved rate performance, and better cycling stability, making such composites ideal for advanced energy storage devices as shown in Fig. 7 and 8.[22,197–200] Scholl *et al.* developed Langmuir–Blodgett films with phospholipid–GO/MnO_2 specifically, *via* simple ultrasonication processing. This method is notable for being low-cost, energy-efficient, and operable at relatively low temperatures.[133] Lohar *et al.* found enhanced specific capacitance in rGO nanosheets upon incorporation of CuO. The inclusion of copper redox ions has been shown to reduce charge transfer resistance. The elevated electrochemical performance of rGO/CuO can be attributed to the synergistic effect of graphene and metal oxide along with the reduced resistance.[171] In another article, Veeresh *et al.* studied the effects of cobalt oxide on rGO.[201] Co_3O_4 is ideal for supercapacitors due to its high redox activity, fast charge transfer kinetics, and abundance of electroactive sites from its unique

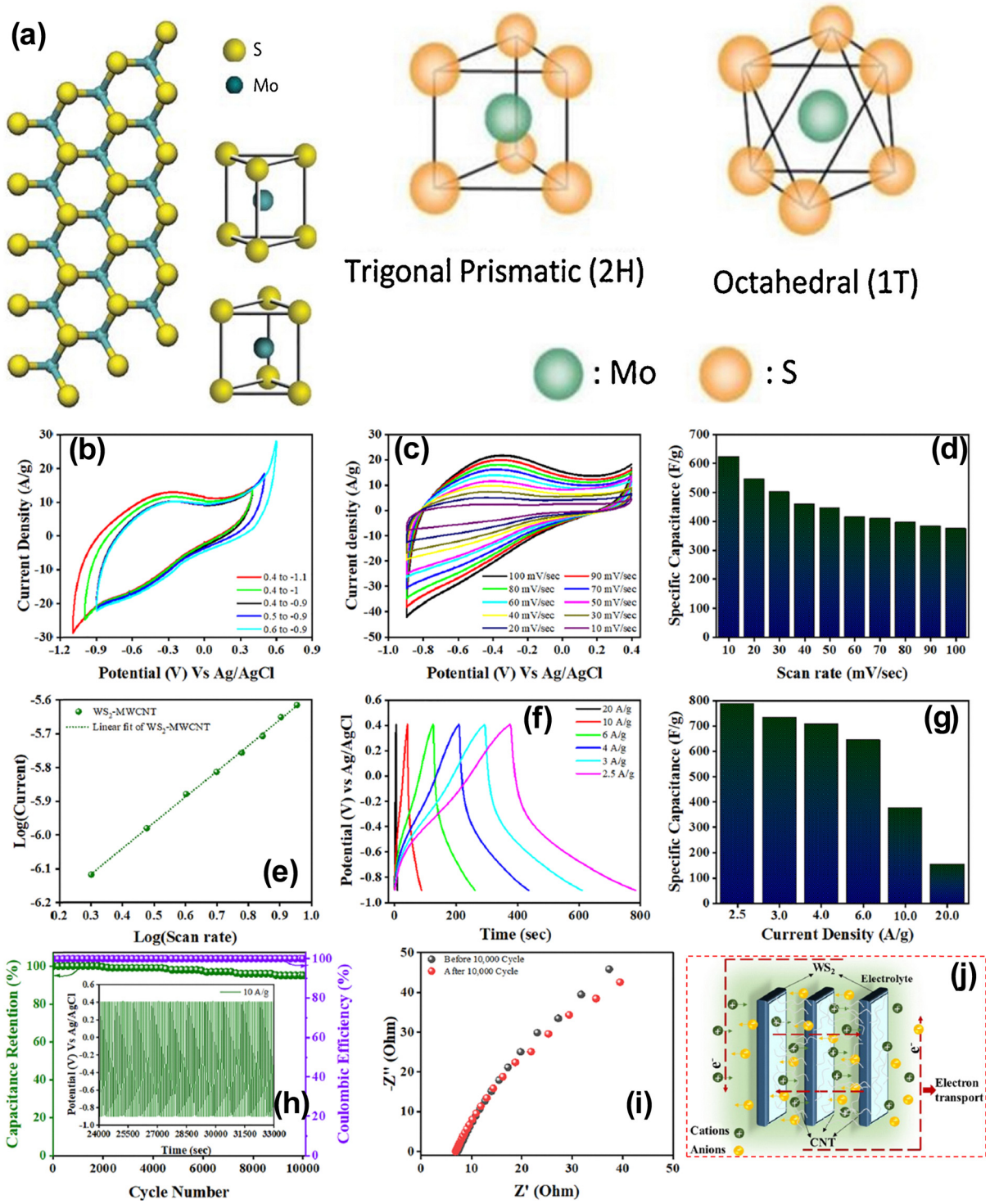

Fig. 6 (a) TMDs crystal structures of MX_2 and three-dimensional model of the MoS_2 crystal structure in 1T and 2H types. Reproduced with permission.[194] CV curves of WS_2–MWCNT supercapacitor at (b) different potential windows, (c) different scan rates, (d) specific capacitance *vs.* scan rates bar chart (e) dependency of power law on peak current (f) GCD curves (g) specific capacitance *vs.* current density bar chart (h) cyclic stability if supercapacitor (i) Nyquist plot before and after 10 000 cycles (j) schematic presentation of WS_2–MWCNT supercapacitor. Reproduced with permission.[182]

spinel structure. Co_3O_4 has Co^{3+} and Co^{2+} oxidation states sited at octahedral and interstitial tetrahedral sites induced by oxygen ions in a tightly packed face-centered cubic structure, respectively. This arrangement in rGO/CuO hybrid supercapacitors offers elevated charge transfer capabilities and high power and energy densities. Hydrothermally synthesized GO/Co_3O_4 showed a maximum C_{sp} value of 1012 F g^{-1} at a current density of 2 A g^{-1}.

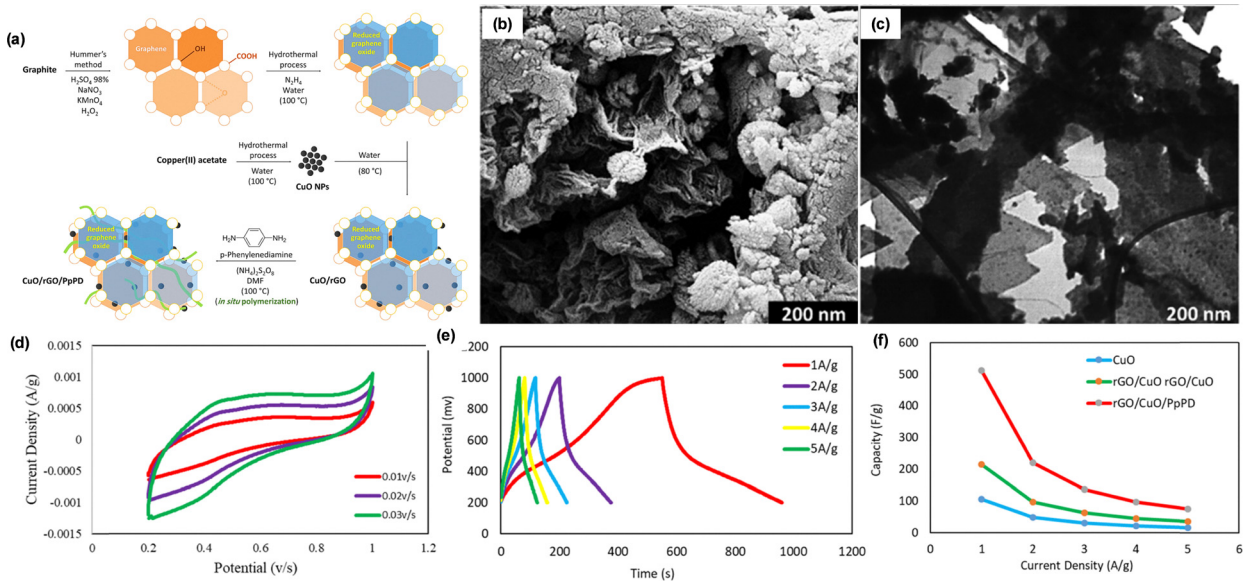

Fig. 7 (a) Schematic illustrations of the preparation route of the rGO/CuO/PpPD ternary nanocomposite. (b) SEM image of rGO/CuO/PpPD nanocomposite. (c) TEM image of rGO/CuO/PpPD nanocomposite. (d) CV curves, (e) GCD curves, and (f) specific capacitance *vs.* current density changes of CuO, rGO/CuO, and rGO/CuO/PpPd electrodes. Reproduced with permission.[170]

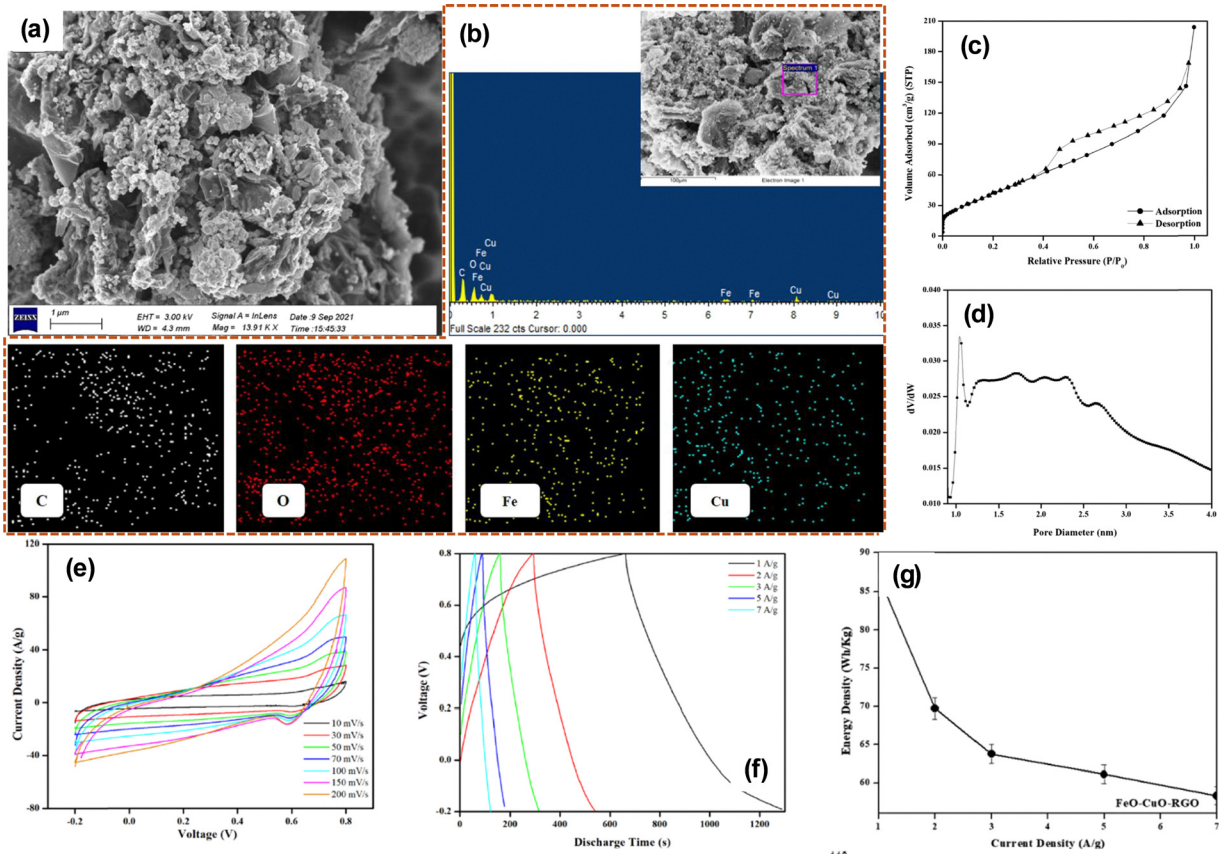

Fig. 8 (a) SEM image and (b) EDS of FeO–CuO–RGO. (c) N_2 adsorption/desorption curve and (d) average pore diameter circulation (e) CV curves (f) GCD curves (g) specific capacitance *vs.* current density plot of FeO–CuO–RGO. Reproduced with permission.[173]

6. Effect of doping

Graphene and it's derivative are ideal candidates in terms of electrode materials for supercapacitors owing to their layered structure, excellent electrical conductivity, large surface area, and various other unique properties. However, the inherent C_{sp} of these materials can be further improved through surface modifications or doping, which enhance its capacitive performance.[202,203] Introducing dopants into graphene electrode materials can generate additional electrochemically active sites or functional groups, thereby enhancing their performance in energy storage applications.

Doping graphene with heteroatoms has been adopted widely to improve its in-plane electrical conductivity, especially for electrode applications.[204] Common dopants include nitrogen (N) and phosphorus (P) for n-type doping, and boron (B) for p-type doping.[205–207] In N-doped graphene, dopant atoms are typically incorporated in between carbon-lattice in three primary bonding configurations: quaternary (graphitic)-N, pyridinic-N, and pyrrolic-N.[208] Snice N have one excess valence electron than carbon, its incorporation creates electron-rich regions within the carbon framework. For example, pyridinic N binds with two C-atoms and eventually contributes to one p-electron in the delocalized π system, on the other hand, pyrrolic N contributes to two p-electrons.[204,209] This introduction of additional charge carriers significantly enhances the electrical conductivity of graphene. Furthermore, N doping alters the charge dispersal and spin-density within the C-arrangement, generating so-called "activation regions" that enhance both the catalytic and electrochemical activity of graphene. Experimental results and theoretical studies suggest that pyridinic and pyrrolic nitrogen species are particularly effective in contributing to pseudocapacitance, thus increasing the overall capacitance. In contrast, quaternary nitrogen primarily boosts electronic conductivity.[210,211]

Graphene and its derivatives are considered highly promising electrode materials due to their 2D or layered structure, exceptional electrical, mechanical and thermal properties, and large theoretical specific surface area. Though, the inherent C_{sp} value of rGO can be modified *via* various modification strategies such as functionalization, doping, which augment its capacitive performance.[202,203] Introducing dopants or functionalisation into graphene electrode materials can generate additional electrochemically active sites or functional groups, thereby enhancing their performance in energy storage applications.

Yuan *et al.* reported that after doping with N, P, and Ni, the specific and gravimetric capacitance of graphene enhanced significantly. The synergistic doping of N, P, and Ni introduces structural defects, enhances active sites, and improves ion transport, collectively boosting capacitance, surface area, and electrochemical performance of graphene.[212] Verma *et al.* reported Fermi-level tuning in h-MoO_3-doped graphene (Fig. 9). MoO_3 molecular doping enables the incorporation of a high hole density in graphene, reaching approximately 2.29×10^{12} cm^{-2}. Additionally, graphene doped with h-MoO_3 exhibits significantly improved supercapacitor performance, achieving an areal capacitance nearly three times greater than that of undoped graphene.[213]

7. Effect of electrolytes

In past few decades, extensive attention has been paid on evaluating the electrochemical performance of electrode

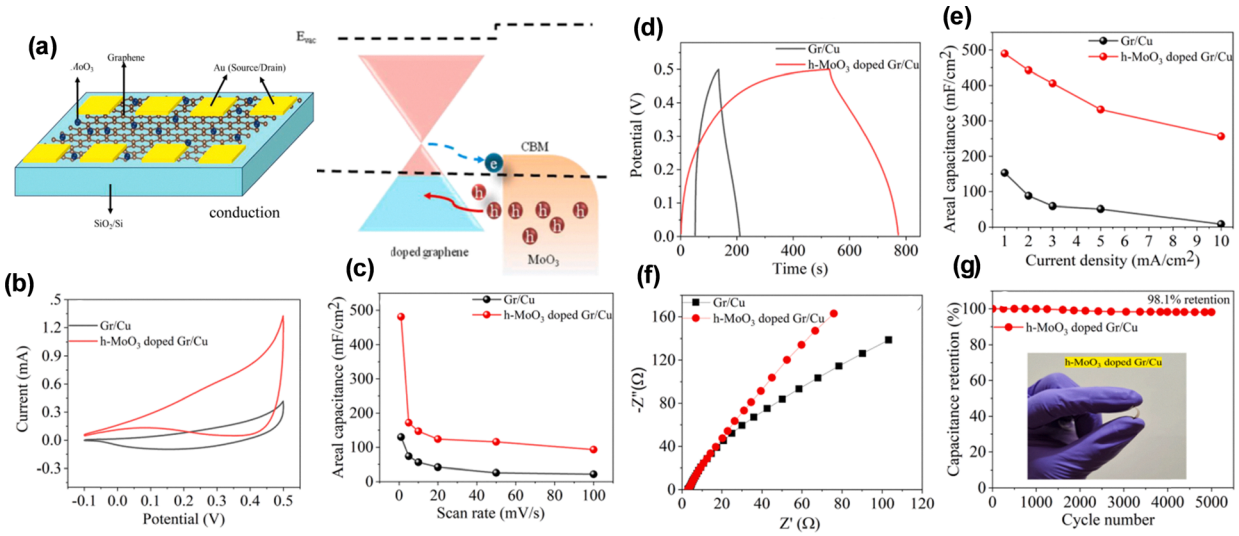

Fig. 9 (a) Schematic representation of fabricated devices of MoO_3-doped CVD grown single layer graphene (SLG) and energy level diagram of graphene/MoO_3 heterostructure. (b) CV curves of pristine graphene on copper foil (Gr/Cu) and h-MoO_3 (1.5 mg mL^{-1}) doped graphene on copper foil (h-MoO_3-doped Gr/Cu) at a scan rate of 10 mV s^{-1} in 2 M KOH electrolyte. (c) Areal capacitance of Gr/Cu and h-MoO_3 doped Gr/Cu as a function of scan rates. (d) GCD curve for Gr/Cu and h-MoO_3-doped Gr/Cu at a current density of 1 mA cm^{-2}. (e) Areal capacitance *versus* current density of Gr/Cu and h-MoO_3-doped Gr/Cu. (f) Nyquist plots of Gr/Cu and h-MoO_3 doped Gr/Cu. (g) Cycling stability test and optical image (inset) of flexible h-MoO_3 doped Gr/Cu electrode. Reproduced with permission.[213]

materials using various electrolytes to enhance their suitability for commercial supercapacitor applications. The key characteristics of a perfect electrolyte includes wide potential window with electrochemical stability, under electrochemical conditions, low internal resistance, and minimal toxicity.[214] Electrolytes generally fall into three main categories: liquid, solid-state, and redox-active, which are further divided into their subcategories as shown in Fig. 10. Selection of an ideal electrolyte is essential to optimize the performance of the supercapacitor, as it significantly affects the potential operating voltage, energy storage capability, and safety of the system (Fig. 11). In this area, the major and existing challenge is identifying electrolytes that can maintain stability over a wide voltage range, given that the voltage window heavily influences both energy density and C_{sp}.[215] Effective electrolytes are also characterized as highly ion-conductive and with the tendency to establish a robust interface with the electrode materials. It is important to avoid electrolyte decomposition, as it can degrade electrode performance. Notably, in studies it has been found that hydrogen electrosorption at the negative electrode can improve both voltage range and C_{sp} values.[216–218]

Aqueous electrolytes are broadly classified into three categories: acidic, basic, and neutral, with H_2SO_4, KOH, and Na_2SO_4 being the most commonly employed representatives of each category, respectively.[155,182,201,219] Although aqueous systems theoretically offer a maximum electrochemical potential window of approximately 1.2 V, in practical applications, this value is often lower, particularly in acidic and alkaline media. Such limitations in voltage window inherently restrict the energy density achievable by supercapacitors utilizing aqueous electrolytes, rendering them less suitable for commercial applications where higher energy densities are required. In contrast, organic electrolytes can sustain much broader voltage windows, offering a distinct advantage in this regard.[220] The productivity

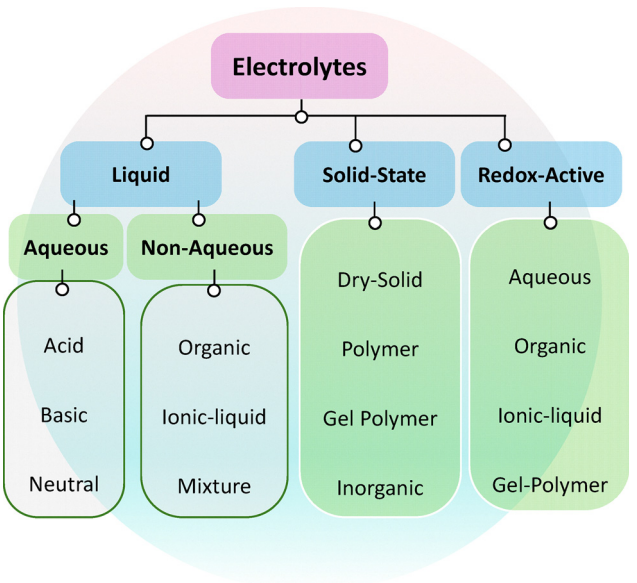

Fig. 10 Classification of electrolytes for supercapacitors.

of aqueous electrolytes is meaningfully prejudiced by parameters such as the ionic-radii of hydrated and bare ions, their mobility, and the nature of ion transport, all of which govern both the C_{sp} and ionic conductivity of the system. Among neutral aqueous electrolytes, potential windows as high as 2.2 V have been documented.[214,221,222]

Organic (non-aqueous) electrolyte-based supercapacitors typically employ a solution comprising a conductive salt, for example tetraethylammonium tetrafluoroborate ($TEABF_4$), that dissolved in organic solvents like polycarbonate or acetonitrile.[223,224] Although widely utilized in commercial supercapacitor technologies, organic electrolytes present several drawbacks, including relatively low ionic conductivity and C_{sp}, high cost, and safety concerns stemming from their toxicity, flammability, and volatility.[225] Furthermore, handling these electrolytes requires stringent purification protocols under controlled atmospheric conditions to prevent moisture contamination, making their processing more complex compared to that of aqueous systems. Despite these limitations, the ability of organic electrolytes to provide an extended electrochemical stability window and enhanced energy density significantly boosts their performance potential. As a result, the adoption of organic electrolyte-based supercapacitors is anticipated to expand, driving increased market demand shortly.[226]

Ionic liquids have appeared as revolutionary electrolytes for supercapacitors thanks to it's ability to support a wider electrochemical potential window compared to traditional electrolytes. These materials offer exceptional attributes, including low flammability, high ionic conductivity (approximately 10 mS cm^{-1}), and excellent chemical stability. While the theoretical potential window ranges between 2 to 6 V, practical applications typically achieve a maximum electrochemical stability of around 4.5 V.[215,227] Unlike conventional electrolytes, ionic liquids do not possess a solvation shell, allowing for a well-defined ion size and a solvent-free environment.[228] A commonly used example in supercapacitor applications is bis(fluorosulfonyl)imide ($[FSI]^-$) anions. Nevertheless, designing ionic liquids that maintain high conductivity and broad voltage ranges across diverse temperatures remains a significant challenge. Ongoing research efforts continue to focus on optimizing these parameters to enhance their suitability for next-generation energy storage systems.[228]

Polymer-based electrolytes have recently gained significant attention for enhancing the electrochemical performance of supercapacitors, primarily owing to their favorable conductance and electrochemical robustness. These are generally categorized as dry-solid, plasticized, and gel polymer electrolytes.[229] Dry-solid polymer electrolytes, often referred to as polymer–salt complexes which works on the principle of dissolution of inorganic salts into polar polymers. This interaction leads to the formation of ion-conducting solid matrices where coordination bonding and electrostatic forces between metal cations and the polar functional groups of the polymer play a critical role.[229] The performance of such systems is significantly affected by multiple parameters. These include the polymer's molecular weight, the chemical composition and

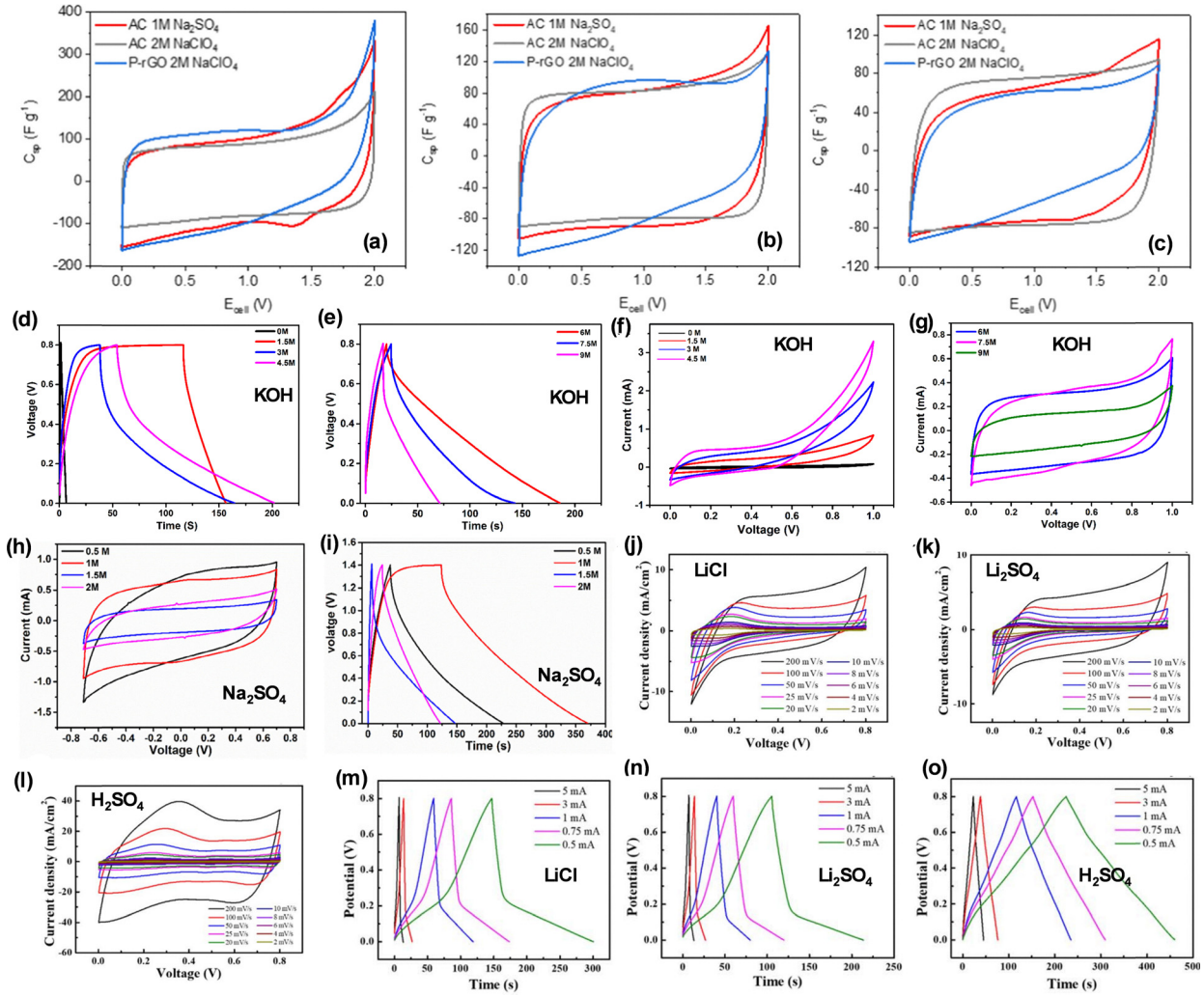

Fig. 11 CV curves of P-rGO and AC in neutral and different electrolytes at different scan rate of (a) 1 mV s^{-1} (b) 10 mV s^{-1} (c) and 50 mV s^{-1}. Reproduced with permission.[240] (d) and (e) GCD curves of RGO for different molar concentrations of KOH at 0.5 A g^{-1}. CV curves of RGO for (f) 0, 1.5, 3 and 4.5 M, (g) 6, 7.5 and 9 M concentrations of KOH at 10 mV s^{-1}. Reproduced with permission.[140] (h) CV curves of RGO in 0.5, 1, 1.5 and 2 M concentrations of Na_2SO_4 at 10 mV s^{-1} (i) GCD curves of RGO supercapacitor in different molarities of Na_2SO_4 at 0.5 A g^{-1}. Reproduced with permission.[141] CV curves of rGO-PANI in (j) LiCl, (k) Li_2SO_4, (l) H_2SO_4. GCD curves of rGO-PANI in (m) LiCl, (n) Li_2SO_4, (o) H_2SO_4. Reproduced with permission.[241]

spacing of its functional groups, the characteristics of the moieties linked to the polymer chain, the nature of counter-ions, and the extent of polymer branching. All these parameters contribute significantly to the strength and nature of polymer–metal ion interactions, ultimately affecting ionic conductivity and overall electrolyte performance.[230–232] Another category of polymer electrolytes employed in supercapacitor systems is plasticized polymer electrolytes. These are typically formulated by incorporating low molecular weight compounds into a polymer framework. Common additives include polyethylene glycol or carbonate-based solvents such as ethylene carbonate and propylene carbonate.[233–235] Despite their enhanced ionic conductivity, plasticized polymer electrolytes often suffer from compromised mechanical strength at elevated levels of plasticization. Additional limitations include the potential reactivity of polar solvents with lithium metal anodes in rechargeable batteries and the volatility of the incorporated solvents. To mitigate these issues, gel polymer electrolytes have been developed. These systems utilize a polymer framework to entrap liquid components, thereby improving safety and mechanical integrity. Although gel polymer electrolytes exhibit relatively better ionic conductance, challenges chemical interaction between polar solvents and metallic electrodes, as well as the emission of volatile substances under certain conditions.[236–239]

8. Challenges and future outlook

Graphene-based electrodes have shown great promise in supercapacitors and other energy storage systems, yet several challenges still hinder their large-scale application. A major limitation is the scalable and cost-effective production of high-quality graphene. Traditional methods like CVD, Hummers' method, and mechanical exfoliation often face issues with yield, consistency, and cost, making them unsuitable for

industrial use. To address this, research focuses on green, low-cost, and high-throughput synthesis techniques such as solvent-free processing, biomass-derived precursors, and continuous flow systems. Another critical challenge is ensuring long-term stability under real-world conditions. In energy storage, graphene-based electrodes can suffer from structural degradation and conductivity loss over time. Enhancing interfacial compatibility, developing hybrid barrier systems, and integrating self-healing properties are key strategies to improve durability. The use of artificial intelligence (AI) and machine learning (ML) is also emerging as a powerful tool for accelerating graphene-based electrodes development. These technologies can optimize material design, predict performance, and reduce experimental workload, provided robust datasets and integrated workflows are established. Looking ahead, the multifunctionality of graphene-based electrodes combining energy storage, mechanical strength, and smart responsiveness positions them as ideal candidates for next-generation applications such as wearable supercapacitors, and structural batteries. Achieving this vision will require materials that are not only high-performing but also durable, flexible, and environmentally resilient.

9. Conclusion

The study and development of 2D materials, specifically graphene and their derivatives, have significantly advanced through technological progress, impacting various fields including energy storage. Graphene's exceptional characteristics include promising thermal and electrical conductivity, large surface area, mechanical robustness, and fast charge–discharge rates make it an ideal material for supercapacitor electrodes. However, challenges like restacking of graphene layers can hinder accessibility and overall performance. To address this, combining graphene with other materials such as carbon composites, metal oxides, or conductive polymers has emerged as a promising strategy. These hybrid composites can reduce particle size, introduce controlled porosity, prevent agglomeration, enhance the number of active sites, and improve both capacitance and cycling stability through additional pseudocapacitive contributions. Future research should continue focusing on the design and optimization of such composites, including ternary systems, to fully harness graphene's capabilities. Moreover, integrating nanoarchitectonic principles could further advance material structuring at the nanoscale, enabling better control over electrochemical behavior. Despite these advancements, several obstacles remain before commercialization, such as ensuring scalability, reproducibility, material stability, and cost-effectiveness. Addressing these challenges is vital for transitioning graphene-based technologies from the lab to practical, real-world energy storage and conversion systems.

Conflicts of interest

The authors declare that they have no known competing financial interests or personal relationships that could have appeared to influence the work reported in this paper.

Data availability

Data sharing is not applicable to this article.

References

1 M. Amir, *et al.*, Energy storage technologies: An integrated survey of developments, global economical/environmental effects, optimal scheduling model, and sustainable adaption policies, *J. Energy Storage*, 2023, **72**, 108694.
2 A. Aghmadi and O. A. Mohammed, Energy storage systems: technologies and high-power applications, *Batteries*, 2024, **10**(4), 141.
3 M. Jafari, A. Botterud and A. Sakti, Decarbonizing power systems: A critical review of the role of energy storage, *Renewable Sustainable Energy Rev.*, 2022, **158**, 112077.
4 S. M. Mousavi, *et al.*, Recent advances in energy storage with graphene oxide for supercapacitor technology, *Sustainable Energy Fuels*, 2023, **7**(21), 5176–5197.
5 Z. Gan, *et al.*, Advances in design of copper-based nanostructures and nanocomposites for high-performance supercapacitors, *J. Energy Storage*, 2024, **99**, 113383.
6 M. E.-S. M. Essa, *et al.*, Improving Micro-Grid Management: A Review of Integration of Supercapacitor across Different Operating Modes, *Heliyon*, 2025, **11**(3), e42178.
7 C. Chetri, *et al.*, Energy Storage Systems for Transportation Electrification, *Electric Vehicles and Distributed Generation-Microgrid*, River Publishers, 2025, pp. 1–38.
8 R. Liang, *et al.*, Transition metal oxide electrode materials for supercapacitors: a review of recent developments, *Nanomaterials*, 2021, **11**(5), 1248.
9 S. Rajagopal, *et al.*, Electrode materials for supercapacitors in hybrid electric vehicles: challenges and current progress, *Condens. Matter*, 2022, **7**(1), 6.
10 S. Karmakar, *et al.*, Review: 2D MXenes based electrochemical sensors and supercapacitors for biomedical and energy storage applications, *Mater. Chem. Phys.*, 2025, **343**, 130974.
11 F. Ahmad, *et al.*, Advances in graphene-based electrode materials for high-performance supercapacitors: A review, *J. Energy Storage*, 2023, **72**, 108731.
12 M. Zafar, *et al.*, Graphene-based polymer nanocomposites for energy applications: Recent advancements and future prospects, *Results Phys.*, 2024, 107655.
13 S. Tamang, *et al.*, A concise review on GO, rGO and metal oxide/rGO composites: Fabrication and their supercapacitor and catalytic applications, *J. Alloys Compd.*, 2023, **947**, 169588.
14 R. Chaturvedi and A. Garg, Environment-friendly approach to rGO–TMD composite synthesis for use as a supercapacitor, *Bull. Mater. Sci.*, 2024, **47**(3), 220.
15 G. K. Gupta, *et al.*, Hydrothermally synthesized nickel ferrite nanoparticles integrated reduced graphene oxide nanosheets as an electrode material for supercapacitors, *J. Mater. Sci.: Mater. Electron.*, 2024, **35**(3), 255.

16 G. K. Gupta, *et al.*, In situ fabrication of activated carbon from a bio-waste desmostachya bipinnata for the improved supercapacitor performance, *Nanoscale Res. Lett.*, 2021, **16**(1), 85.
17 A. Kumar, *et al.*, A sensitive SPR biosensor for glucose detection using MoS2 quantum dots, *Microchem. J.*, 2025, **214**, 113889.
18 A. Yadav, *et al.*, A smartphone-enabled colorimetric sensor based on VS2 quantum dots for Rapid and on-site detection of ferric ions, *Spectrochim. Acta, Part A*, 2025, **329**, 125609.
19 P. Sagar, *et al.*, WS2 nanoparticle integrated MWCNT as an efficient electrode material for electrochemical sensing of chloramphenicol in pharmaceutical samples, *Microchem. J.*, 2025, **210**, 112922.
20 G. Perozziello, *et al.*, Nature Inspired Plasmonic Structures: Influence of Structural Characteristics on Sensing Capability, *Appl. Sci.*, 2018, **8**(5), 668.
21 A. Ganguly, *et al.*, Controlling Vertical Asymmetry of Nanocrystals Through Anisotropic Etching-Assisted Nanosphere Lithography, *Small Struct.*, 2024, **5**(3), 2300300.
22 G. K. Gupta, *et al.*, Excellent supercapacitive performance of graphene quantum dots derived from a bio-waste marigold flower (Tagetes erecta), *Int. J. Hydrogen Energy*, 2021, **46**(77), 38416–38424.
23 S. Mishra, *et al.*, The impact of physicochemical features of carbon electrodes on the capacitive performance of supercapacitors: a machine learning approach, *Sci. Rep.*, 2023, **13**(1), 6494.
24 T. Zhang and F. Ran, Design strategies of 3D carbon-based electrodes for charge/ion transport in lithium ion battery and sodium ion battery, *Adv. Funct. Mater.*, 2021, **31**(17), 2010041.
25 S. Jang, *et al.*, Multiscale Architectured Membranes, Electrodes, and Transport Layers for Next-Generation Polymer Electrolyte Membrane Fuel Cells, *Adv. Mater.*, 2023, **35**(43), 2204902.
26 A. Ganguly and G. Das, Combining azimuthal and polar angle resolved shadow mask deposition and nanosphere lithography to uncover unique nano-crystals, *Nanomaterials*, 2022, **12**(19), 3464.
27 A. Bouzina, *et al.*, Preventing graphene from restacking *via* bioinspired chemical inserts: toward a superior 2D micro-supercapacitor electrode, *ACS Appl. Nano Mater.*, 2021, **4**(5), 4964–4973.
28 K. Pramoda and C. Rao, Electrostatic restacking of two-dimensional materials to generate novel hetero-superlattices and their energy applications, *APL Mater.*, 2023, **11**(2), 020901.
29 H. Zhang, *et al.*, Hybridized graphene for supercapacitors: Beyond the limitation of pure graphene, *Small*, 2021, **17**(12), 2007311.
30 Y. Li, *et al.*, Flexible β-Ni(OH)2/graphene electrode with high areal capacitance enhanced by conductive interconnection, *J. Alloys Compd.*, 2018, **737**, 731–739.
31 S. Hussain, *et al.*, WS2-embedded MXene/GO hybrid nanosheets as electrodes for asymmetric supercapacitors and hydrogen evolution reactions, *Chem. Eng. J.*, 2023, **452**, 139523.
32 S. Mitra, *et al.*, High-performance solar-blind flexible deep-UV photodetectors based on quantum dots synthesized by femtosecond-laser ablation, *Nano Energy*, 2018, **48**, 551–559.
33 J. Huang, *et al.*, Rational design of electrode materials for advanced supercapacitors: from lab research to commercialization, *Adv. Funct. Mater.*, 2023, **33**(14), 2213095.
34 X. Jiang, *et al.*, The impact of electrode with carbon materials on safety performance of lithium-ion batteries: a review, *Carbon*, 2022, **191**, 448–470.
35 C. V. Pham, *et al.*, Essentials of high performance water electrolyzers–from catalyst layer materials to electrode engineering, *Adv. Energy Mater.*, 2021, **11**(44), 2101998.
36 S. Mahmud, *et al.*, Recent advances in lithium-ion battery materials for improved electrochemical performance: A review, *Results Eng.*, 2022, **15**, 100472.
37 X. Zhu, Recent advances of transition metal oxides and chalcogenides in pseudo-capacitors and hybrid capacitors: A review of structures, synthetic strategies, and mechanism studies, *J. Energy Storage*, 2022, **49**, 104148.
38 A. G. Olabi, *et al.*, Supercapacitors as next generation energy storage devices: Properties and applications, *Energy*, 2022, **248**, 123617.
39 A. Dutta, *et al.*, A comprehensive review on batteries and supercapacitors: Development and challenges since their inception, *Energy Storage*, 2023, **5**(1), e339.
40 C. Lamiel, *et al.*, Properties, functions, and challenges: current collectors, *Mater. Today Chem.*, 2022, **26**, 101152.
41 M. Mondal, D. K. Goswami and T. K. Bhattacharyya, High-performing asymmetric 2 V supercapacitor assembled with leucine-capped rGO-α-Fe2O3 as anode and PANI decorated mwCNT-V2O5 as cathode, *J. Electrochem. Soc.*, 2023, **170**(11), 110521.
42 J. Singh, *et al.*, Synthesis of activated N/O/S-codoped porous carbon from waste sugarcane bagasse cellulose for high energy density solid-state asymmetric supercapacitors, *J. Ind. Eng. Chem.*, 2025, **147**, 793–807.
43 E. P. da Silva, *et al.*, Sustainable energy and waste management: How to transform plastic waste into carbon nanostructures for electrochemical supercapacitors, *Waste Manage.*, 2023, **171**, 71–85.
44 A. Srivastava, *et al.*, Investigating the thermodynamics properties of water confined in carbon nanotubes using molecular dynamics simulations, *Sci. Rep.*, 2025, **15**(1), 21574.
45 G. Das, *et al.*, Few molecule SERS detection using nanolens based plasmonic nanostructure: application to point mutation detection, *RSC Adv.*, 2016, **6**(109), 107916–107923.
46 N. M. Sadiq, *et al.*, Advancements in green polymer blend nanocomposite electrolytes (PPBNEs) and activated carbon for EDLC application with high energy density, *J. Energy Storage*, 2024, **93**, 112282.
47 S. J. Panchu, K. Raju and H. C. Swart, Emerging Two–Dimensional Intercalation Pseudocapacitive Electrodes

for Supercapacitors, *ChemElectroChem*, 2024, **11**(15), e202300810.
48 K. Kim, *et al.*, Ultrafast PEDOT: PSS/H2SO4 electrical double layer capacitors: comparison with polyaniline pseudocapacitors, *ChemSusChem*, 2023, **16**(5), e202202057.
49 M. Sarno, Nanotechnology in energy storage: the supercapacitors, in *Studies in Surface Science and Catalysis*, ed. A. Basile, *et al.*, Elsevier, 2020, pp. 431–458.
50 D. Nimmakayala, S. Srivastava and S. Kumar, Self-discharge in supercapacitors. Part I: Conway's diagnostics, *Wiley Interdiscip. Rev.:Energy Environ.*, 2024, **13**(2), e515.
51 A. Khan, *et al.*, Highly redox active mesoporous Ni/Co-organic framework as a potential battery type electrode material for high energy density supercapattery, *J. Energy Storage*, 2023, **58**, 106317.
52 J. A. Goudar, *et al.*, Cobalt-Based Materials in Supercapacitors and Batteries: A Review, *Adv. Energy Sustainability Res.*, 2025, **6**(2), 2400271.
53 R. Liu, *et al.*, Fundamentals, advances and challenges of transition metal compounds-based supercapacitors, *Chem. Eng. J.*, 2021, **412**, 128611.
54 P. Bhojane, Recent advances and fundamentals of Pseudocapacitors: Materials, mechanism, and its understanding, *J. Energy Storage*, 2022, **45**, 103654.
55 T. Ramachandran, *et al.*, Asymmetric supercapacitors: Unlocking the energy storage revolution, *J. Energy Storage*, 2023, **73**, 109096.
56 S. Karmakar, *et al.*, 1D rod-like mixed Ni–Co–Mo metallic oxide anchored on Ni foam as a novel positrode for high energy density asymmetric supercapacitors, *Electrochim. Acta*, 2025, **536**, 146797.
57 J. Huang, K. Yuan and Y. Chen, Wide Voltage Aqueous Asymmetric Supercapacitors: Advances, Strategies, and Challenges, *Adv. Funct. Mater.*, 2022, **32**(4), 2108107.
58 T. Ramachandran, *et al.*, Asymmetric supercapacitors: Unlocking the energy storage revolution, *J. Energy Storage*, 2023, **73**, 109096.
59 N. Wu, *et al.*, Recent advances of asymmetric supercapacitors, *Adv. Mater. Interfaces*, 2021, **8**(1), 2001710.
60 S. V. Sadavar, S. Y. Lee and S. J. Park, Advancements in asymmetric supercapacitors: from historical milestones to challenges and future directions, *Adv. Sci.*, 2024, **11**(34), 2403172.
61 S. Alipoori, S. H. Aboutalebi and M. Barsbay, Enhancing the performance of solid-state supercapacitors: Optimizing the molecular interactions in flexible gel polymer electrolytes, *J. Solid State Electrochem.*, 2024, **28**(8), 2643–2657.
62 L. A. Garcés-Patiño, *et al.*, Maximizing the Electrochemical Performance of Supercapacitors by Using Seawater Electrolyte Instead of Acidic/Lithium-Based Electrolytes, *Adv. Sustainable Syst.*, 2025, **9**(3), 2400668.
63 S. B. Aziz, *et al.*, Steps towards the ideal CV and GCD results with biodegradable polymer electrolytes: plasticized MC based green electrolyte for EDLC application, *J. Energy Storage*, 2024, **76**, 109730.
64 V. Molahalli, *et al.*, Renewable Musa Sapientum derived porous nano spheres for efficient energy storage devices, *Nano Express*, 2024, **5**(3), 035006.
65 Y. Xu, J. Li and W. Huang, Porous Graphene Oxide Prepared on Nickel Foam by Electrophoretic Deposition and Thermal Reduction as High-Performance Supercapacitor Electrodes, *Materials*, 2017, **10**(8), 936.
66 H. S. Magar, R. Y. Hassan and A. Mulchandani, Electrochemical impedance spectroscopy (EIS): Principles, construction, and biosensing applications, *Sensors*, 2021, **21**(19), 6578.
67 Y. Wang, Y. Song and Y. Xia, Electrochemical capacitors: mechanism, materials, systems, characterization and applications, *Chem. Soc. Rev.*, 2016, **45**(21), 5925–5950.
68 H. V. T. Nguyen, *et al.*, Size effect of electrolyte ions on the electric double-layer structure and supercapacitive behavior, *ACS Appl. Energy Mater.*, 2023, **6**(5), 3155–3166.
69 C. Mevada, *et al.*, Bio-inspired 3D-Printed supercapacitors for sustainable energy storage, *J. Power Sources*, 2024, **624**, 235529.
70 R. N. A. R. Seman, M. A. Azam and M. H. Ani, Graphene/transition metal dichalcogenides hybrid supercapacitor electrode: status, challenges, and perspectives, *Nanotechnology*, 2018, **29**(50), 502001.
71 F. Wang, *et al.*, Latest advances in supercapacitors: from new electrode materials to novel device designs, *Chem. Soc. Rev.*, 2017, **46**(22), 6816–6854.
72 G. Gupta, *et al.*, Fabrication of manganese ferrite-reduced graphene oxide nanostructure as an electrode material for high performance supercapacitor, *Emergent Mater.*, 2024, **7**(4), 1475–1487.
73 L. Xie, *et al.*, Effect of pore structure and doping species on charge storage mechanisms in porous carbon-based supercapacitors, *Mater. Chem. Front.*, 2020, **4**(9), 2610–2634.
74 Q. Wu, *et al.*, Cyclic stability of supercapacitors: materials, energy storage mechanism, test methods, and device, *J. Mater. Chem. A*, 2021, **9**(43), 24094–24147.
75 A. K. Ghasemi, *et al.*, Facile synthesize of PANI/GO/CuFe2O4 nanocomposite material with synergistic effect for superb performance supercapacitor, *Electrochim. Acta*, 2023, **439**, 141685.
76 H. Gul, A.-U.-H. A. Shah and S. Bilal, Achieving ultrahigh cycling stability and extended potential window for supercapacitors through asymmetric combination of conductive polymer nanocomposite and activated carbon, *Polymers*, 2019, **11**(10), 1678.
77 M. Pathak, S. M. Jeong and C. S. Rout, Graphene hybrids for supercapacitor applications, *Chem. Commun.*, 2025, **61**, 8803–8829.
78 X. Tian, Q. Zhu and B. Xu, ''Water-in-salt'' electrolytes for supercapacitors: A review, *ChemSusChem*, 2021, **14**(12), 2501–2515.
79 Z. Ali Zafar, *et al.*, Aqueous Supercapacitor with Wide-Temperature Operability and over 100 000 Cycles Enabled by Water-in-Salt Electrolyte, *ChemSusChem*, 2025, **18**(6), e202401681.

80 D. Qu, *et al.*, Electrochemical impedance and its applications in energy-storage systems, *Small Methods*, 2018, **2**(8), 1700342.
81 M. Catelani, *et al.*, Experimental characterization of hybrid supercapacitor under different operating conditions using EIS measurements, *IEEE Trans. Instrum. Meas.*, 2023, **73**, 1–10.
82 X. Tao, *et al.*, ATMP doped conductive PANI/CNTs composite hydrogel electrodes toward high energy density flexible supercapacitors, *ACS Appl. Energy Mater.*, 2023, **6**(15), 8177–8188.
83 B. Akkinepally, *et al.*, Promising electrode material of Fe3O4 nanoparticles decorated on V2O5 nanobelts for high-performance symmetric supercapacitors, *Ceram. Int.*, 2023, **49**(4), 6280–6288.
84 M. He, *et al.*, Potential Specific Adsorption of Electrolyte Components Induced by Point Defected Graphene in EDLCs: A DFT Research, *ChemistrySelect*, 2025, **10**(1), e202404711.
85 M. T. T. Moghadam, *et al.*, ZnWO4-CNT as a superior electrode material for ultra-high capacitance supercapacitor, *Surf. Interfaces*, 2022, **32**, 102134.
86 A. Tyagi, *et al.*, Performance studies of an electric double-layer capacitor (EDLC) fabricated using edible oil-derived activated carbon, *J. Mater. Sci.: Mater. Electron.*, 2022, **33**(11), 8920–8934.
87 G. Sharma, *et al.*, Activated carbon as superadsorbent and sustainable material for diverse applications, *Adsorpt. Sci. Technol.*, 2022, **2022**, 4184809.
88 M. M. Mohamed, *et al.*, A Comprehensive Evaluation of Biomass-Derived Activated Carbon Materials for Electrochemical Applications in Zinc-Ion Hybrid Supercapacitors, *ACS Appl. Energy Mater.*, 2024, **7**(17), 7517–7533.
89 S. Sameera, *et al.*, Enhanced wide spectrum photocatalytic activity by in-situ magnetite-graphite nanoplatelets heterostructure, *IEEE Access*, 2023, **11**, 68912–68924.
90 G. Das, *et al.*, Plasmonic nanostructures for the ultrasensitive detection of biomolecules, *La Riv.Nuovo Cimento*, 2016, **39**(11), 547–586.
91 M. Zhong, M. Zhang and X. Li, Carbon nanomaterials and their composites for supercapacitors, *Carbon Energy*, 2022, **4**(5), 950–985.
92 S. Simon, *et al.*, Carbon Nanotubes for Supercapacitors, *NanoCarbon: A Wonder Material for Energy Applications: Fundamentals and Advancement for Energy Storage Applications*, Springer, 2024, pp. 217–236, vol. 2.
93 D. D. Chronopoulos, *et al.*, Carbon nanotube based metal–organic framework hybrids from fundamentals toward applications, *Small*, 2022, **18**(4), 2104628.
94 X. Liu, *et al.*, Tungsten oxide-based nanomaterials for supercapacitors: Mechanism, fabrication, characterization, multifunctionality, and electrochemical performance, *Prog. Mater. Sci.*, 2022, **130**, 100978.
95 M. Khot and A. Kiani, A review on the advances in electrochemical capacitive charge storage in transition metal oxide electrodes for pseudocapacitors, *Int. J. Energy Res.*, 2022, **46**(15), 21757–21796.
96 M. H. Gharahcheshmeh and K. U. A. Chowdhury, Fabrication methods, pseudocapacitance characteristics, and integration of conjugated conducting polymers in electrochemical energy storage devices, *Energy Adv.*, 2024, 2668–2703.
97 M. G. Saborio, *et al.*, Polymer/reduced graphene oxide/lignosulfonate nanocomposite films as pseudocapacitor cathodes, *ACS Appl. Nano Mater.*, 2022, **5**(3), 3686–3700.
98 W. Jian, *et al.*, Engineering pore nanostructure of carbon cathodes for zinc ion hybrid supercapacitors, *Adv. Funct. Mater.*, 2022, **32**(49), 2209914.
99 J. Joyner, *et al.*, Graphene supported MoS2 structures with high defect density for an efficient HER electrocatalysts, *ACS Appl. Mater. Interfaces*, 2020, **12**(11), 12629–12638.
100 G. Kucinskis, G. Bajars and J. Kleperis, Graphene in lithium ion battery cathode materials: A review, *J. Power Sources*, 2013, **240**, 66–79.
101 W. Bi, *et al.*, Surface immobilization of transition metal ions on nitrogen-doped graphene realizing high-efficient and selective CO2 reduction, *Adv. Mater.*, 2018, **30**(18), 1706617.
102 U. Harini and C. Ponraj, Graphene-based electrochemical sensors for detecting environmental pollutants, *J. Electrochem. Soc.*, 2024, **171**(2), 027521.
103 R. Sha, *Graphene-based electrochemical sensors for environmental monitoring applications*, 2023.
104 R. Samal, S. Radhakrishnan and C. S. Rout, Analytical techniques for pore size and specific surface area analysis, *Advanced Analytical Techniques for Characterization of 2D Materials*, 2022.
105 R. B. Onyancha, *et al.*, A methodical review on carbon-based nanomaterials in energy-related applications, *Adsorpt. Sci. Technol.*, 2022, **2022**, 4438286.
106 S. A. L. Sameera, *et al.*, Enhanced Wide Spectrum Photocatalytic Activity by in-Situ Magnetite-Graphite Nanoplatelets Heterostructure, *IEEE Access*, 2023, **11**, 68912–68924.
107 G. Das, *et al.*, Graphene: A building foundation for efficient plasmonic sers device. Biochem, *Biochem. Anal. Biochem.*, 2017, **6**(01), 1–6.
108 C. Wang, *et al.*, Graphene's role in emerging trends of capacitive energy storage, *Small*, 2021, **17**(48), 2006875.
109 Y. Wang, *et al.*, Planar Micro-Supercapacitors with High Power Density Screen-Printed by Aqueous Graphene Conductive Ink, *Materials*, 2024, **17**(16), 4021.
110 A. S. Reddy, *et al.*, EDL Supercapacitor Electrode Performance Analysis of Group-VIB and Group-X Transition Metal Adsorbed and Doped Graphene: A Density Functional Theory Based Comparative Investigation, *ACS Appl. Electron. Mater.*, 2024, **6**(7), 5301–5313.
111 A. Gutiérrez-Cruz, *et al.*, A review of top-down and bottom-up synthesis methods for the production of graphene, graphene oxide and reduced graphene oxide, *J. Mater. Sci.*, 2022, **57**(31), 14543–14578.
112 E. T. Mombeshora and E. Muchuweni, Dynamics of reduced graphene oxide: synthesis and structural models, *RSC Adv.*, 2023, **13**(26), 17633–17655.

113 H. Komal Zafar, *et al.*, Recent Advances on Nitrogen-doped Porous Carbons Towards Electrochemical Supercapacitor Applications, *Chem. Rec.*, 2024, **24**(1), e202300161.
114 V. K. Kumar and N. Panwar, A review on porous carbon synthesis processes and its application as energy storage supercapacitor, *J. Indian Chem. Soc.*, 2024, 101231.
115 D. Mani, *et al.*, Recent Advances in Structural Designs and Fabrication of Flexible Polymer Composites Films with High Thermal Conductivity and Electromagnetic Interference Shielding Performance, *J. Mater. Chem. C*, 2025, **13**, 8890–8933.
116 Z. Liu, G. Xiang and S. Zhang, Carbon Fibers, *Carbon Catalysis*, CRC Press, 2024, pp. 302–350.
117 A. Agrawal, Top-down strategies for achieving high-quality graphene: recent advancements, *J. Ind. Eng. Chem.*, 2024, 103–126.
118 S. Devi, *et al.*, Graphene and Its Derivatives: Various Routes of Synthesis, *Electrochemical Exfoliation of Graphene and Its Derivatives: Commercial Applications*, Springer, 2024, pp. 61–112.
119 A. Saravanan, *et al.*, Insights on synthesis and applications of graphene-based materials in wastewater treatment: A review, *Chemosphere*, 2022, **298**, 134284.
120 J. Amontree, *et al.*, Reproducible graphene synthesis by oxygen-free chemical vapour deposition, *Nature*, 2024, **630**(8017), 636–642.
121 S. H. Kim, *et al.*, Ultralow-temperature ultrafast synthesis of wafer-scale single-crystalline graphene *via* metal-assisted graphitization of silicon-carbide, *arXiv*, 2025, preprint, arXiv:2502.17799, DOI: **10.48550/arXiv.2502.17799**.
122 R. Kumar, *et al.*, Laser processing of graphene and related materials for energy storage: State of the art and future prospects, *Prog. Energy Combust. Sci.*, 2022, **91**, 100981.
123 M. Farshadnia, *et al.*, Facile synthesis of NiTe2-Co2Te2@ rGO nanocomposite for high-performance hybrid supercapacitor, *Sci. Rep.*, 2023, **13**(1), 1364.
124 T. Chen, *et al.*, In situ synthesis of Ni-BTC metal–organic framework@ graphene oxide composites for high-performance supercapacitor electrodes, *ACS Omega*, 2023, **8**(12), 10888–10898.
125 Z. Wang, *et al.*, Growth of two-dimensional covalent organic frameworks on substrates: insight from microsecond atomistic simulations, *Chem. Sci.*, 2024, **15**(42), 17629–17641.
126 M. Zhao, C. Casiraghi and K. Parvez, Electrochemical exfoliation of 2D materials beyond graphene, *Chem. Soc. Rev.*, 2024, 3036–3064.
127 J. Aixart, *et al.*, Increasing reaction time in Hummers' method towards well exfoliated graphene oxide of low oxidation degree, *Ceram. Int.*, 2021, **47**(15), 22130–22137.
128 X. Lin, *et al.*, In situ growth of graphene on both sides of a Cu–Ni alloy electrode for perovskite solar cells with improved stability, *Nat. Energy*, 2022, **7**(6), 520–527.
129 N. An, *et al.*, Hierarchical porous covalent organic framework/graphene aerogel electrode for high-performance supercapacitors, *J. Mater. Chem. A*, 2021, **9**(31), 16824–16833.
130 Y. Yan, *et al.*, Synthesis of graphene oxide and graphene quantum dots from miscanthus *via* ultrasound-assisted mechano-chemical cracking method, *Ultrason. Sonochem.*, 2021, **73**, 105519.
131 C. Li, *et al.*, Scalable combustion synthesis of graphene-welded activated carbon for high-performance supercapacitors, *Chem. Eng. J.*, 2021, **414**, 128781.
132 V. T. Le, *et al.*, Simultaneous enhancement of specific capacitance and potential window of graphene-based electric double-layer capacitors using ferroelectric polymers, *J. Power Sources*, 2021, **507**, 230268.
133 F. A. Scholl, *et al.*, Exploring Langmuir-Blodgett films with phospholipid-graphene oxide/MnO2 as a hybrid nanostructured interface for supercapacitor applications, *Colloids Surf., A*, 2023, **664**, 131128.
134 H. Zhao, *et al.*, A Highly Capacitive Graphene/Multiholed N-CNTs Hybrid Evolved from Black Humate-Co-melamine Precursor, *ChemNanoMat*, 2025, **11**(1), e202400492.
135 A. Imbrogno, *et al.*, Laser-Induced Graphene Supercapacitors by Direct Laser Writing of Cork Natural Substrates, *ACS Appl. Electron. Mater.*, 2022, **4**(4), 1541–1551.
136 R. Correia, *et al.*, Biocompatible Parylene-C Laser-Induced Graphene Electrodes for Microsupercapacitor Applications, *ACS Appl. Mater. Interfaces*, 2022, **14**(41), 46427–46438.
137 P. A. Le, *et al.*, Food seasoning-derived gel polymer electrolyte and pulse-plasma exfoliated graphene nanosheet electrodes for symmetrical solid-state supercapacitors, *RSC Adv.*, 2022, **12**(3), 1515–1526.
138 B. Bai, *et al.*, Copper Phosphosulfide Nanosheets on Cu-Coated Graphene Fibers as Asymmetric Supercapacitor Electrodes, *ACS Appl. Nano Mater.*, 2024, **7**(11), 12387–12398.
139 H. Huang, *et al.*, Three-dimensional porous reduced graphene oxide/PEDOT:PSS aerogel: Facile preparation and high performance for supercapacitor electrodes, *Electrochim. Acta*, 2020, **364**, 137297.
140 P. Krishnan and V. Biju, Effect of electrolyte concentration on the electrochemical performance of RGO–KOH supercapacitor, *Bull. Mater. Sci.*, 2021, **44**(4), 288.
141 P. Krishnan and V. Biju, Effect of electrolyte concentration on the electrochemical performance of RGO-Na2SO4 supercapacitor, *Mater. Today: Proc.*, 2022, **54**, 958–962.
142 F. Qu, *et al.*, Hierarchical polypyrrole/graphene/melamine composite foam for highly compressible all-solid-state supercapacitors, *Electrochim. Acta*, 2020, **353**, 136600.
143 Y. He, X. Ning and L. Wan, Ultrathin graphene oxide@polypyrrole nanosheets as a supercapacitor electrode with high areal specific capacitance, *Polym. Bull.*, 2022, **79**(10), 9075–9091.
144 G. Liu, *et al.*, Reduced graphene oxide/polypyrrole composite: an advanced electrode for high-performance symmetric/asymmetric supercapacitor, *Carbon Lett.*, 2020, **30**(4), 389–397.

145 J. Chen, *et al.*, Pulsed electrochemical fabrication of graphene/polypyrrole composite gel films for high performance and flexible supercapacitors, *Electrochim. Acta*, 2020, **361**, 137036.
146 A. U. H. A. Shah, *et al.*, Reduced Graphene Oxide/Poly(Pyrrole-*co*-Thiophene) Hybrid Composite Materials: Synthesis, Characterization, and Supercapacitive Properties, *Polymers*, 2020, **12**(5), 1110.
147 G. K. Gupta, *et al.*, Fabrication of manganese ferrite-reduced graphene oxide nanostructure as an electrode material for high performance supercapacitor, *Emergent Mater.*, 2024, **7**(4), 1475–1487.
148 G. K. Gupta, *et al.*, Hydrothermally synthesized nickel ferrite nanoparticles integrated reduced graphene oxide nanosheets as an electrode material for supercapacitors, *J. Mater. Sci.: Mater. Electron.*, 2024, **35**(3), 255.
149 S. Zhu, *et al.*, Flash Nitrogen-Doped Graphene for High-Rate Supercapacitors, *ACS Mater. Lett.*, 2022, **4**(10), 1863–1871.
150 B. Liu, *et al.*, Electrochemically exfoliated chlorine-doped graphene for flexible all-solid-state micro-supercapacitors with high volumetric energy density, *Adv. Mater.*, 2022, **34**(19), 2106309.
151 C. S. Bongu, *et al.*, Flexible and Freestanding MoS2/Graphene Composite for High-Performance Supercapacitors, *ACS Omega*, 2023, **8**(40), 36789–36800.
152 M. Serrapede, *et al.*, The combination of MoS2/reduced graphene oxide composite electrode and ionic liquid for high-temperature supercapacitor, *J. Energy Storage*, 2023, **73**, 109180.
153 S. Sardana, *et al.*, Hierarchical flower-like MoS2/reduced graphene oxide nanohybrids supported on nickel foam as a high-performance electrode material for supercapacitor applications, *J. Mater. Chem. A*, 2023, **11**(11), 5910–5924.
154 V. Panwar, *et al.*, Gate Field Induced Extraordinary Energy Storage in MoS2-Graphene-Based Ultramicro-Electrochemical Capacitor, *ACS Energy Lett.*, 2023, **8**(3), 1510–1519.
155 E. Moradpur-Tari, R. Sarraf-Mamoory and A. Yourdkhani, 1T-WS2/Graphene on activated carbon cloth as a flexible electrode for wearable supercapacitors, *Ceram. Int.*, 2022, **48**(6), 8563–8571.
156 T. Feng, *et al.*, Heterolayered 2D Nanohybrids of Graphene-WS2 Nanosheets: Enabling Enhanced Supercapacitive Performance of Polyaniline, *Energy Fuels*, 2023, **37**(8), 6266–6275.
157 S. Sengupta and M. Kundu, All-Solid-State Flexible Asymmetric Supercapacitors Based on WS2/rGO/CNT Hybrid Electrodes and Polymer-Based Ionic Liquid Electrolytes, *ACS Appl. Energy Mater.*, 2024, **7**(9), 4243–4251.
158 X. Yang, *et al.*, NiS2/MoS2 mixed phases with abundant active edge sites induced by sulfidation and graphene introduction towards high-rate supercapacitors, *Chem. Eng. J.*, 2021, **406**, 126713.
159 S. Mondal, U. Rana and S. Malik, Reduced Graphene Oxide/Fe3O4/Polyaniline Nanostructures as Electrode Materials for an All-Solid-State Hybrid Supercapacitor, *J. Phys. Chem. C*, 2017, **121**(14), 7573–7583.
160 F. Hekmat, S. Shahrokhian and N. Taghavinia, Ultralight flexible asymmetric supercapacitors based on manganese dioxide–polyaniline nanocomposite and reduced graphene oxide electrodes directly deposited on foldable cellulose papers, *J. Phys. Chem. C*, 2018, **122**(48), 27156–27168.
161 S. Parwaiz, *et al.*, Cobalt-Doped Ceria/Reduced Graphene Oxide Nanocomposite as an Efficient Oxygen Reduction Reaction Catalyst and Supercapacitor Material, *J. Phys. Chem. C*, 2017, **121**(37), 20165–20176.
162 B. Gangopadhyay, *et al.*, Thermal Effects on Electrochemical Performance of Copper Oxide Nanoparticles Decorated Amine-Functionalized Graphene Oxide for Ultrahigh Energy Density Supercapacitor with Real-Life Application, *J. Phys. Chem. C*, 2023, **127**(45), 21940–21953.
163 A. R. Ansari, *et al.*, Silver nanoparticles embedded on reduced graphene Oxide@ Copper oxide nanocomposite for High Performance Supercapacitor Applications, *Materials*, 2021, **14**(17), 5032.
164 P. J. S. Jennifer, *et al.*, Exploring ternary hybrid nanocomposite of NiO@ CuO embedded on reduced graphene oxide as supercapacitor electrode, *J. Mater. Sci.: Mater. Electron.*, 2023, **34**(8), 727.
165 S. Nagarani, *et al.*, ZnO-CuO nanoparticles enameled on reduced graphene nanosheets as electrode materials for supercapacitors applications, *J. Energy Storage*, 2022, **52**, 104969.
166 S. Yazar, Construction of enriched CuO/Cu2O electrode materials with discrete heteroatom-doped graphene oxide and investigation of capacitance performance for symmetrical supercapacitor application, *Chem. Pap.*, 2023, **77**(9), 5259–5273.
167 D. Khalafallah, *et al.*, Structuring graphene quantum dots anchored CuO for high-performance hybrid supercapacitors, *J. Taiwan Inst. Chem. Eng.*, 2021, **122**, 168–175.
168 S. Ravichandran, *et al.*, Biosynthesis of copper oxide nanoparticle from clerodendrum phlomidis and their decoration with graphene oxide for photocatalytic and supercapacitor application, *J. Mater. Sci.: Mater. Electron.*, 2022, **33**(12), 9403–9411.
169 S. V. Chandran and B. N. Narayanan, Copper oxide incorporated ball-mill produced less-defective graphene for hybrid supercapacitors, *Diamond Relat. Mater.*, 2024, **143**, 110842.
170 R. Eivazzadeh-Keihan, *et al.*, Effective Combination of rGO and CuO Nanomaterials through Poly(p-phenylenediamine) Texture: Utilizing It as an Excellent Supercapacitor, *Energy Fuels*, 2021, **35**(13), 10869–10877.
171 G. M. Lohar, O. C. Pore and A. V. Fulari, Electrochemical behavior of CuO/rGO nanopellets for flexible supercapacitor, non-enzymatic glucose, and H2O2 sensing application, *Ceram. Int.*, 2021, **47**(12), 16674–16687.
172 R. Kandulna, *et al.*, Assessment of dielectrical and electrochemical properties of PPY:CuO:rGO nanocomposite for organic light-emitting diodes and supercapacitor applications, *J. Mater. Sci.: Mater. Electron.*, 2025, **36**(5), 337.

173 M. Rahaman, *et al.*, Iron Oxide- and Copper Oxide-Decorated Chemically Reduced Graphene Oxide Composite as a Novel Electrode for Hybrid Supercapacitors, *Energy Fuels*, 2022, **36**(7), 3976–3986.
174 J. Vigneshwaran, *et al.*, Fe2O3 decorated graphene oxide/polypyrrole matrix for high energy density flexible supercapacitor, *Surf. Interfaces*, 2021, **27**, 101572.
175 D. Mohanadas, *et al.*, A promising negative electrode of asymmetric supercapacitor fabricated by incorporating copper-based metal-organic framework and reduced graphene oxide, *Int. J. Hydrogen Energy*, 2021, **46**(71), 35385–35396.
176 S. Z. Golkhatmi, *et al.*, One-step electrodeposition synthesis of high performance Graphene/Cu2O nanocomposite films on copper foils as binder-free supercapacitor electrodes, *Solid State Sci.*, 2020, **106**, 106336.
177 R. Ghanbari, *et al.*, Iron (II and III) Oxides/Reduced Graphene Oxide/Polypyrrole Ternary Nanocomposite as Electrochemical Supercapacitor Electrode, *J. Electrochem. Soc.*, 2021, **168**(3), 030543.
178 S. Yousaf, *et al.*, Hierarchically porous CuO microspheres and their r-GO based nanohybrids for electrochemical supercapacitors applications, *J. Mater. Res. Technol.*, 2020, **9**(6), 14158–14167.
179 Y. Dong, *et al.*, α-Fe2O3/rGO nanospindles as electrode materials for supercapacitors with long cycle life, *Mater. Res. Bull.*, 2018, **107**, 391–396.
180 A. Aldalbahi, *et al.*, Reduced graphene oxide supersonically sprayed on wearable fabric and decorated with iron oxide for supercapacitor applications, *J. Mater. Sci. Technol.*, 2021, **82**, 47–56.
181 S. S. Magdum, S. Thangarasu and T. H. Oh, Three-Dimensional Ternary rGO/VS2/WS2 Composite Hydrogel for Supercapacitor Applications, *Inorganics*, 2022, **10**(12), 229.
182 F. Mashkoor, *et al.*, Freestanding WS2-MWCNT Nanocomposite for Electrochemical Detection of Contaminants of Emerging Concern–Perfluorooctanoic Acid ''A Forever Chemical'' and Supercapacitor Applications, *ACS Sustainable Chem. Eng.*, 2023, **11**(36), 13306–13319.
183 P. Sagar, M. Srivastava and S. Srivastava, Boron functionalized and phosphorous doped molybdenum di-sulfide quantum dots for the photoluminescence based detection of HbA1c, *Microchem. J.*, 2024, **207**, 111885.
184 A. Kumar, *et al.*, A sensitive SPR biosensor for glucose detection using MoS2 quantum dots, *Microchem. J.*, 2025, 113889.
185 X. Xu, *et al.*, High-Performance Monolayer MoS2 Films at the Wafer Scale by Two-Step Growth, *Adv. Funct. Mater.*, 2019, **29**(32), 1901070.
186 P. Sagar, *et al.*, The fabrication of an MoS2 QD–AuNP modified screen-printed electrode for the improved electrochemical detection of cefixime, *Anal. Methods*, 2020, **12**(23), 3014–3024.
187 G. Perozziello, *et al.*, Nanoplasmonic and microfluidic devices for biological sensing, *Nano-Optics: Principles Enabling Basic Research and Applications*, Springer, 2017, pp. 247–274.
188 Z. Thiehmed, A. Shakoor and T. Altahtamouni, Recent advances in WS2 and its based heterostructures for water-splitting applications, *Catalysts*, 2021, **11**(11), 1283.
189 H. Li, *et al.*, Subgroup discovery points to the prominent role of charge transfer in breaking nitrogen scaling relations at single-atom catalysts on VS2, *ACS Catal.*, 2021, **11**(13), 7906–7914.
190 M. A. Kosnan, *et al.*, Recent progress of electrode architecture for MXene/MoS2 supercapacitor: preparation methods and characterizations, *Micromachines*, 2022, **13**(11), 1837.
191 R. Sha, *et al.*, Review—MoSe2 Nanostructures and Related Electrodes for Advanced Supercapacitor Developments, *J. Electrochem. Soc.*, 2022, **169**(1), 013503.
192 S. K. Balasingam, J. S. Lee and Y. Jun, Molybdenum diselenide/reduced graphene oxide based hybrid nanosheets for supercapacitor applications, *Dalton Trans.*, 2016, **45**(23), 9646–9653.
193 Y. Zhuo, *et al.*, Self-assembled 1T-MoS2/functionalized graphene composite electrodes for supercapacitor devices, *ACS Appl. Energy Mater.*, 2022, **5**(1), 61–70.
194 M.-h Wu, *et al.*, Molybdenum disulfide (MoS2) as a co-catalyst for photocatalytic degradation of organic contaminants: A review, *Process Saf. Environ. Prot.*, 2018, **118**, 40–58.
195 T. Tene, *et al.*, Role of graphene oxide and reduced graphene oxide in electric double-layer capacitors: A systematic review, *Batteries*, 2024, **10**(7), 256.
196 T. Schötz, *et al.*, Disentangling faradaic, pseudocapacitive, and capacitive charge storage: a tutorial for the characterization of batteries, supercapacitors, and hybrid systems, *Electrochim. Acta*, 2022, **412**, 140072.
197 B. Ying, *et al.*, Effective carrier doping and quantum capacitance manipulation of graphene through two-dimensional solid electrolytes of ScI3 and YBr3, *Appl. Surf. Sci.*, 2023, **616**, 156443.
198 S. Gupta, *et al.*, Perspectives on electron transfer kinetics across graphene-family nanomaterials and interplay of electronic structure with defects and quantum capacitance, *Sci. Rep.*, 2025, **15**(1), 1–27.
199 A. Kanwade and P. M. Shirage, A review on synergy of transition metal oxide nanostructured materials: Effective and coherent choice for supercapacitor electrodes, *J. Energy Storage*, 2022, **55**, 105692.
200 A. Shah, *et al.*, Supercapacitor performance of NiO, NiO-MWCNT, and NiO–Fe-MWCNT composites, *ACS Omega*, 2023, **8**(37), 33380–33391.
201 S. Veeresh, *et al.*, Graphene oxide/cobalt oxide nanocomposite for high-performance electrode for supercapacitor application, *J. Energy Storage*, 2022, **52**, 104715.
202 D. Prakash and S. Manivannan, N, B co-doped and crumpled graphene oxide pseudocapacitive electrode for high energy supercapacitor, *Surf. Interfaces*, 2021, **23**, 101025.

203 M. B. Arvas, M. Gencten and Y. Sahin, One-step synthesized N-doped graphene-based electrode materials for supercapacitor applications, *Ionics*, 2021, **27**, 2241–2256.
204 M. S. K. Chowdury, *et al.*, Two-dimensional nanostructured pristine graphene and heteroatom-doped graphene-based materials for energy conversion and storage devices, *Sustainable Mater. Technol.*, 2024, e01124.
205 Y.-S. Chang, *et al.*, N-doped reduced graphene oxide for room-temperature NO gas sensors, *Sci. Rep.*, 2021, **11**(1), 20719.
206 P. M. Pandian and A. Pandurangan, Flexible asymmetric solid-state supercapacitor of boron doped reduced graphene for high energy density and power density in energy storage device, *Diamond Relat. Mater.*, 2021, **118**, 108495.
207 R. Thomas and M. Balachandran, Fuel coke derived nitrogen and phosphorus co-doped porous graphene structures for high-performance supercapacitors: The trail towards a brown-to-green transition, *J. Energy Storage*, 2023, **72**, 108799.
208 N. Talukder, *et al.*, Nitrogen-doped graphene nanomaterials for electrochemical catalysis/reactions: A review on chemical structures and stability, *Carbon*, 2021, **185**, 198–214.
209 P. Zhao, *et al.*, Effect of nitrogen species on electrochemical properties of N-doped carbon nanotubes derived from co-pyrolysis of low-density polyethylene and melamine, *J. Energy Storage*, 2023, **67**, 107569.
210 W. Zhu, D. Shen and H. Xie, Effect of heteroatoms on pseudocapacitance for N/O Co-doped porous carbon in an alkaline aqueous electrolyte, *Energy Fuels*, 2023, **37**(16), 12467–12473.
211 R. Sánchez-Salas, *et al.*, Effect of pyrrolic-N defects on the capacitance and magnetization of nitrogen-doped multiwalled carbon nanotubes, *Carbon*, 2021, **183**, 743–762.
212 Z. Yuan, *et al.*, N-, P-, and Ni-Co-doped Porous Carbon from Poplar Powder and Graphene Oxide Composites as Electrode Materials for Supercapacitors, *Energy Fuels*, 2023, **37**(3), 2420–2430.
213 V. Verma, *et al.*, Fermi-level tuning in graphene *via* green synthesized h-MoO3: Enhanced supercapacitor performance of h-MoO3 doped graphene, *J. Alloys Compd.*, 2025, **1018**, 179225.
214 X. Fan, *et al.*, Opportunities of flexible and portable electrochemical devices for energy storage: expanding the spotlight onto semi-solid/solid electrolytes, *Chem. Rev.*, 2022, **122**(23), 17155–17239.
215 M. Saha, *et al.*, A comprehensive review of novel emerging electrolytes for supercapacitors: Aqueous and organic electrolytes versus ionic liquid-based electrolytes, *Energy Fuels*, 2024, **38**(10), 8528–8552.
216 K. Fic, *et al.*, Comparative operando study of degradation mechanisms in carbon-based electrochemical capacitors with Li2SO4 and LiNO3 electrolytes, *Carbon*, 2017, **120**, 281–293.
217 H. Yang and N. Wu, Ionic conductivity and ion transport mechanisms of solid-state lithium-ion battery electrolytes: A review, *Energy Sci. Eng.*, 2022, **10**(5), 1643–1671.
218 Y. Pang, *et al.*, Electrolyte/electrode interfaces in all-solid-state lithium batteries: a review, *Electrochem. Energy Rev.*, 2021, **4**, 169–193.
219 T. Bhat, P. Patil and R. Rakhi, Recent trends in electrolytes for supercapacitors, *J. Energy Storage*, 2022, **50**, 104222.
220 Y. Ding, P. Cai and Z. Wen, Electrochemical neutralization energy: from concept to devices, *Chem. Soc. Rev.*, 2021, **50**(3), 1495–1511.
221 S. Yuan, *et al.*, Organic electrode materials for energy storage and conversion: mechanism, characteristics, and applications, *Acc. Chem. Res.*, 2024, **57**(10), 550–1563.
222 P. Kumar and S. Yashonath, Ionic conductivity in aqueous electrolyte solutions: Insights from computer simulations, *J. Mol. Liq.*, 2019, **277**, 506–515.
223 H. V. T. Nguyen and K.-K. Lee, Tetraethylphosphonium tetrafluoroborate electrolyte for paving the way to construct high-power and high-voltage supercapacitors, *J. Energy Storage*, 2024, **96**, 112640.
224 Y. Lai, *et al.*, Tetraethylammonium difluoro (oxalato) borate as electrolyte salt for electrochemical double-layer capacitors, *Electrochim. Acta*, 2011, **56**(18), 6426–6430.
225 T. T. Truong, *et al.*, Conventional supercapacitor electrolytes: aqueous, organic, and ionic, *Supercapacitors*, Elsevier, 2024, pp. 245–265.
226 M. Gaško, *et al.*, Tetraethylammonium Perfluorobutanesulfonate as an Alternative Salt for Electric Double Layer Capacitors, *Batteries Supercaps*, 2024, **7**(11), e202400283.
227 S. Kazemiabnavi, *et al.*, Electrochemical stability window of imidazolium-based ionic liquids as electrolytes for lithium batteries, *J. Phys. Chem. B*, 2016, **120**(25), 5691–5702.
228 J. Pereira, R. Souza and A. Moita, A Review of Ionic Liquids and Their Composites with Nanoparticles for Electrochemical Applications, *Inorganics*, 2024, **12**(7), 186.
229 G. Xi, *et al.*, Polymer-based solid electrolytes: material selection, design, and application, *Adv. Funct. Mater.*, 2021, **31**(9), 2007598.
230 C.-Y. Hui, C.-W. Kan and K.-H. Chau, A study on poly (ethylene oxide)-based supercapacitors doped with various dopants, *Coatings*, 2023, **13**(8), 1373.
231 J. Qin, *et al.*, Preparation of Polyethylene Oxide and Polyvinyl Alcohol Blended Polymer Electrolyte Membrane Using Water as Solvent for Solid-State Supercapacitors, *J. Appl. Polym. Sci.*, 2025, e57165.
232 M. Y. Bhat and S. Hashmi, Mixture of non-ionic and organic ionic plastic crystals immobilized in poly (vinylidene fluoride-*co*-hexafluoropropylene): A flexible gel polymer electrolyte composition for high performance carbon supercapacitors, *J. Energy Storage*, 2022, **51**, 104514.
233 S. Kim, *et al.*, Cross-Linked Composite Gel Polymer Electrolyte Based on an H-Shaped Poly (ethylene oxide)–Poly (propylene oxide) Tetrablock Copolymer with SiO2 Nanoparticles for Solid-State Supercapacitor Applications, *ACS Omega*, 2021, **6**(26), 16924–16933.
234 S. A. Mane, *et al.*, Polyethylene glycol assisted synthesis of V2O5 nanofibers as an efficient electrode material for

symmetric supercapacitors, *J. Mater. Sci.: Mater. Electron.*, 2023, **34**(8), 719.

235 P. Wuamprakhon, *et al.*, Unveiling a Novel Decomposition Pathway in Propylene Carbonate-Based Supercapacitors: Insights from a Jelly Roll Configuration Study, *ChemSusChem*, 2024, **17**(18), e202400053.

236 L. Lv, *et al.*, Lamellar agarose/graphene oxide gel polymer electrolyte network for all-solid-state supercapacitor, *Chem. Eng. J.*, 2023, **452**, 139443.

237 M. Ghasemi, *et al.*, Porous gel polymer electrolyte for the solid state metal oxide supercapacitor with a wide potential window, *J. Taiwan Inst. Chem. Eng.*, 2021, **118**, 223–231.

238 J. Yang, *et al.*, Tough and redox-mediated alkaline gel polymer electrolyte membrane for flexible supercapacitor with high energy density and low temperature resistance, *J. Membr. Sci.*, 2022, **650**, 120386.

239 H. Duan, *et al.*, Tough, highly adaptable and self-healing integrated supercapacitor based on double network gel polymer electrolyte, *Energy*, 2023, **264**, 126244.

240 K. Gajewska, *et al.*, Effect of electrolyte and carbon material on the electrochemical performance of high-voltage aqueous symmetric supercapacitors, *J. Mater. Sci.*, 2023, **58**(4), 1721–1738.

241 W.-H. Cho, I. C. Cheng and J.-Z. Chen, Performance Comparison of Reduced Graphene Oxide (rGO)-polyaniline (PANI) Supercapacitors with LiCl, Li2SO4, and H2SO4 Electrolytes, *J. Electrochem. Soc.*, 2023, **170**(1), 010532.